Transmit Precoding for Interference Exploitation in the Underlay Cognitive Radio Z-channel

Ka Lung Law, *Student Member, IEEE*, Christos Masouros, *Senior Member, IEEE*, and Marius Pesavento, *Member, IEEE*

***Abstract*—This paper introduces novel transmit precoding approaches for the cognitive radio (CR) Z-channel. The proposed transmission schemes exploit noncausal information about the interference at the secondary base station to redesign the CR precoding optimization problem. This is done with the objective to improve the quality of service (QoS) of secondary users by taking advantage of constructive interference in the secondary link. The precoders are designed to minimize the worst secondary user's symbol error probability (SEP) under constraints on the instantaneous total transmit power, and the power of the instantaneous interference in the primary link. The problem is formulated as a bivariate probabilistic constrained programming (BPCP) problem. We show that the BPCP problem can be transformed for practical SEPs into a convex optimization problem that can be solved, for example, by the barrier method. A computationally efficient tight approximate approach is also developed to compute the near-optimal solutions. Simulation results and analysis show that the average computational complexity per downlink frame of the proposed approximate problem is comparable to that of the conventional CR downlink beamforming problem. In addition, both the proposed methods offer significant performance improvements as compared to the conventional CR downlink beamforming, while guaranteeing the QoS of primary users on an instantaneous basis, in contrast to the average QoS guarantees of conventional beamformers.**

***Index Terms*—Downlink beamforming, cognitive radio, constructive interference, bivariate probabilistic constrained programming, convex optimization.**

I. Introduction

DYNAMIC spectrum access (DSA) in cognitive radio (CR) networks has provided an effective way to increase the radio resource utilization and spectral efficiency, by allowing the utilization of the licensed spectrum by secondary links [1]–[5]. In underlay CR networks, the primary users (PUs) have the highest priority to access the spectrum without being aware of the existence of the unlicensed secondary user (SU) network. However, under the underlay CR paradigm the PU network is willing to grant spectrum access to the SU network under the premise that the interference created by the secondary base station (SBS) does not exceed a predefined threshold [4]. With the knowledge of channel state information (CSI) for both the PUs and SUs at the SBS, a fundamental challenge for CR is to enable opportunistic spectrum access while meeting the quality of service (QoS) requirements of the SUs, e.g., in terms of signal to interference plus noise ratio (SINR), system capacity, or symbol error rate (SER). The policy of CR network in return guarantees to protect the PUs from interference induced by the SUs [5]–[7].

To facilitate the utilization of the available radio spectrum, CR employs techniques from traditional (non-CR) wireless networks [5]. Existing studies in the traditional networks have shown that the QoS can be improved by exploiting the spatial domain with the use of multiple antennas at the SBS [8], [9]. Several beamforming techniques haven been developed for the conventional wireless downlink to amplify the signal and suppress the interference by exploiting the CSI [8]–[16]. With the introduction of pre-coding techniques, multiuser downlink designs have been developed extensively in non-CR wireless communications. Dirty paper coding (DPC) techniques have been introduced to pre-eliminating potential interference experienced at the receiver already before transmission [17], [18]. However, the DPC techniques, despite being capacity optimal, involve non-linear and non-continuous optimization, which require sophisticated search algorithms and assume the data are encoded by codewords with infinite length [19]. Several heuristic approaches are proposed to reduce the complexity [20]–[22]. Nevertheless, they are generally far from being practical in current communication standards due to high computational complexity.

As regards the CR transmission, the power minimization and SINR balancing problem for SUs with average interference power constraints of the primary users has been discussed in [5], [23]. Conventionally this problem is solved by (sequential) approximation as of second-order cone programs (SOCPs). To achieve more flexibility than that of the worst-case based design, channel outage univariate probabilistic constrained programming (UPSP) downlink beamforming problem has been

Manuscript received October 7, 2016; revised January 25, 2017 and March 24, 2017; accepted April 10, 2017. Date of publication May 2, 2017; date of current version May 16, 2017. The associate editor coordinating the review of this manuscript and approving it for publication was Prof. Mats Bengtsson. The work of C. Masouros was supported in part by the Royal Academy of Engineering, U.K., and in part the Engineering and Physical Sciences Research Council (EPSRC) Project EP/M014150/1. *(Corresponding author: Christos Masouros.)*

K. L. Law and C. Masouros are with the Department of Electronic and Electrical Engineering, University College London, London WC1E 7JE, U.K. (e-mail: k.law@ucl.ac.uk; chris.masouros@ieee.org).

M. Pesavento is with the Communication Systems Group, Technische Universität Darmstadt, Darmstadt D-64283, Germany (e-mail: mpesa@nt.tu-darmstadt.de).

Color versions of one or more of the figures in this paper are available online at http://ieeexplore.ieee.org.

Digital Object Identifier 10.1109/TSP.2017.2695448

developed [24], [25]. Nevertheless, the techniques of solving for UPSP problem could not be extended to multivariate probabilistic constrained programming problem as the problem is non-convex in general [26].

In order to improve the performance, the above mentioned SINR-based CR downlink beamforming problems are designed to mitigate the multiuser interference among the SUs. However, the associated drawback is that in SINR-based designs, some degrees of freedom in the beamforming design are used to suppress and eliminate the interference, which results in an overall increase of the transmitted power. Moreover, with conventional CR beamforming [5], [23], which only constrains the average interference, the instantaneous interference at the PUs at individual time instants may largely exceed the predefined thresholds. This can be overcome by utilizing the knowledge of both CSI and SU's information symbols at the SBS to exploit the resulting interference in the secondary links. In this case beamformers can be designed to enhance the useful signal by steering the received signals, containing both the desired and the interfering signals, into the correct detection region instead of separately amplifying and suppressing the desired and the interfering signals, respectively [21], [27]–[37]. Related to this concept, recent work focuses on the topic of transmitter side precoding for physical-layer security by means of directional modulation. This technique exploits the constellation formats to distort the receive signals at potential eavesdroppers on a symbol-by-symbol basis, which leads to high error rate on the eavesdropper side [38]–[42]. This approach is also known as a constructive interference precoding. Closed-form linear and non-linear constructive interference precoders were developed for the non-CR downlink to achieve higher SINRs at the receivers without the requirement of additional transmit power as compared to the interference suppression techniques [21], [27], [29], [30], [34], [35]. To further reduce the transmit power, the beamforming optimization-based precoders are discussed in [36], [37], [43], [44]. Recent work has adapted the above CR precoders based on the concept of constructive inteference [45]. While this work focuses on the CR X-channel, here our focus is on the Z-channel.

The above works, build upon the observation that in time division duplexing (TDD) systems, downlink channels CSI can be obtained from uplink training due to the assumption of uplink-downlink channel reciprocity [46]. Thus the training process can be simplified without the feedback of CSI estimate from the receiver. More importantly, by using the constructive interference technique the decoding process can be further simplified. That is, with conventional beamforming the receiver needs to calculate the composite channel (composed by the product of its downlink channel with the corresponding beamformer) for equalization and detection. With the proposed technique however, it will be shown that, as the received symbols fall in the constructive region of the signal constellation, no such equalization is required at the receiver and a simple decision stage at the receiver side suffices. Accordingly, The benefit for the proposed scheme is threefold: 1.) There is no need to send common pilots to the users to estimate the Multiple InputSingle Output (MISO) channels. 2.) There is no need to signal the beamformers for the users compute the composite channels for equalization. 3.) It is not subject to the associated errors in the composite channel due to the estimation errors and CSI quantization during the feedback procedure, which further deteriorate the performance.

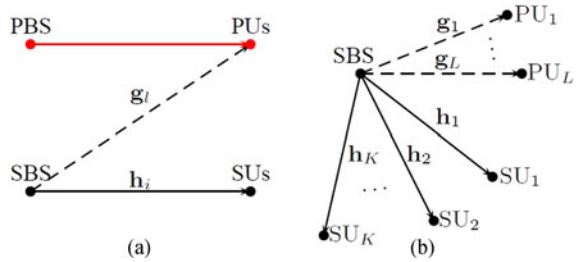

Fig. 1. (a) The basic cognitive Z-channel and (b) The cognitive radio with K SUs and L PUs in SBS network.

In line with the above, this paper extends the work on the downlink precoding optimization problem by exploiting the constructive interference [36], [37], [43] to the CR Z-channel scenarios, which consists of a primary base station (PBS), a single multi-antenna SBS, and multiple single-antenna SUs, where it was previously inapplicable. Vishwanath, Jindal, and Goldsmith [47] introduced the Z-channel shown in Fig. 1(a), in which only the interference from the SBS to the PUs is considered, while the interference from the PBS to the SUs is assumed weak or negligible, which finds practical significance for example when the cognitive receiver is far from the primary transmitter. Alternatively, in the absence of data and channel information from the PBS, it is typically assumed that this interference is incorporated in the noise term that, by use of the central limit theorem, can be modelled as a circularly symmetric complex Gaussian process with zero mean. We assume that the TDD protocol is applied, instantaneous CSI is available at the transmitter and instantaneous SU transmit data information are utilized at the SBS, as in [36], [37], [43]. We further note that, for the purposes of precoding, the SBS can obtain the estimate of the SBS-to-PUs channel through the PU pilot transmission during the training stage of the primary link through reciprocity. We formulate the precoder design problem to minimize the worst SU's symbol error probability (WSUSEP) subject to total transmit power and PU instantaneous interference constraints, where WSUSEP is defined as the probability that worst SU wrongly decodes its symbol. The major contributions of this paper can be summarized as follows:

1) We formulate the WSUSEP precoder design for the CR network that exploits constructive interference within the secondary link, subject to instantaneous interference constraints to the PUs.
2) We derive conditions under which the probabilistic precoding design allows a reformulation as a convex deterministic precoding problem that can be efficiently solved using, e.g., the barrier method and show that these conditions are generally met in practical scenario.
3) We derive a simple and computationally efficient approximation technique with remarkably low computational complexity in terms of average execution time that

achieves close to optimal performance and allows a convenient SOCP reformulation.

All the above algorithms are shown to offer an improved performance-complexity trade-off compared to existing CR beamforming techniques.

Remark 1: The above generic concept of interference exploitation can be applied to a number of related CR beamforming techniques such as the CSI-robust beamformers of [24] amongst others. To constrain our focus on the proposed concept, however, here we concentrate on the CR beamforming of [5], [23], which we use as our reference and main performance benchmark. We designate the application of the constructive interference concept to alternative CR precoders as the focus of our future work.

Remark 2: In the following analysis, we consider the phase-shift keying (PSK) modulation. This is motivated by the fact that our proposed schemes are most suitable for high interference scenarios where typically low order PSK modulations are employed to secure reliable transmission. Nevertheless, by enlarging the correct detection modulation region to exploit constructive interference, it has been shown in [34], [48] that the exploitation of constructive interference can be extended to other modulation schemes such as quadrature amplitude modulation (QAM). In further work, we are looking forward to extending our proposed constructive interference-based approaches to QAM using the similar techniques given in [34], [48].

The remainder of the paper is organized as follows. Section II introduces the signal model and then revisits the conventional CR downlink beamforming problem. In Section III, the constructive interference exploitation is introduced and the WSUSEP-based precoding problem for CR networks is presented. Section IV develops an approximate approach of solving the WSUSEP-based CR downlink precoding problem. Section V provides simulation results. Conclusions are drawn in Section VI.

Notation: $\mathrm{E}\{\cdot\}$, $\Pr(\cdot)$, $|\cdot|$, $\|\cdot\|$, $(\cdot)^*$ $(\cdot)^T$, $\arg(\cdot)$, denote the statistical expectation, the probability function, the absolute value, the Euclidean norm, the complex conjugate, and the transpose, the angle in a complex plane between the positive real axis to the line joining the point to the origin, respectively. $\mathbf{I}_j$, and $\mathbf{0}_{j,j}$ denotes the $j \times j$ identity matrix, and $j \times j$ zero matrix, respectively. mod is defined to be the modulo operation. $\mathrm{blkdiag}(\mathbf{a}_1, \ldots, \mathbf{a}_n)$ is the block diagonal matrix where $\mathbf{a}_i$ are on main diagonal blocks such that the off-diagonal blocks are zero matrices. $\mathrm{Re}(\cdot)$ and $\mathrm{Im}(\cdot)$ are the real part, and the imaginary part, respectively.

II. System Model and Conventional Downlink Beamforming Problem

We consider a single cell CR Z-channel system, which consists of a single N-antenna SBS, K single-antenna SUs and L single-antenna PUs shown in Fig. 1(b). The signal transmitted by the SBS is given by the $N \times 1$ vector

$$\mathbf{x} = \sum_{i=1}^{K} \mathbf{w}_i b_i, \tag{1}$$

where $b_i \triangleq e^{j\vartheta_i}$ is the unit amplitude M-order PSK (M-PSK) modulated symbol, $\vartheta_i \triangleq i\pi/M$ is the phase of the constellation point for ith transmit data symbol, and $\mathbf{w}_i$ is the $N \times 1$ beamforming weight vector for the ith SU. Let $\mathbf{h}_i$ be the $N \times 1$ channel vector from SBS to the ith SU. The received signal of the ith SU is

$$y_i = \mathbf{h}_i^T \mathbf{x} + n_i = \underbrace{\mathbf{h}_i^T \mathbf{w}_i b_i}_{\text{desired signal}} + \underbrace{\sum_{j=1, j\neq i}^{K} \mathbf{h}_i^T \mathbf{w}_j b_j + n_i}_{\text{interference plus noise}}, \tag{2}$$

where n_i at the ith SU is a circularly symmetric complex Gaussian with zero mean, i.e., $n_i \sim \mathcal{CN}(0, \sigma^2)$ and σ^2 is the noise variance for all SUs. In [5]–[23], it is common to assume the independence of the symbols transmitted to different users, i.e., $\mathrm{E}\{b_j^* b_i\} = 0$ for $i \neq j$. The received SINR for the ith SU is generally expressed as the mean desired signal power over transmit symbols divided by the mean interference over transmit symbols plus noise power [24], i.e.,

$$\begin{aligned} \mathrm{SINR}_i &\triangleq \frac{\mathrm{E}\{|\mathbf{h}_i^T \mathbf{w}_i b_i|^2\}}{\sum_{\substack{j=1 \\ j\neq i}}^{K} \mathrm{E}\{|\mathbf{h}_i^T \mathbf{w}_j b_j|^2\} + \sigma^2} \\ &= \frac{|\mathbf{h}_i^T \mathbf{w}_i|^2}{\sum_{\substack{j=1 \\ j\neq i}}^{K} |\mathbf{h}_i^T \mathbf{w}_j|^2 + \sigma^2}. \end{aligned} \tag{3}$$

The mean interference power over transmit symbols at the lth PU can be written as [5]

$$\begin{aligned} \mathcal{I}_l &= \mathrm{E}\left\{ |\sum_{i=1}^{K} \mathbf{g}_l^T \mathbf{w}_i b_i|^2 \right\} \\ &= \mathrm{E}\left\{ \sum_{j=1}^{K} \sum_{i=1}^{K} b_j^* b_i \mathbf{w}_j{}^H \mathbf{g}_l^* \mathbf{g}_l^T \mathbf{w}_i \right\} = \sum_{i=1}^{K} |\mathbf{g}_l^T \mathbf{w}_i|^2, \end{aligned} \tag{4}$$

where $\mathbf{g}_l$ is the $N \times 1$ channel vector between the SBS and lth PU. The average total transmitted power P_T over transmit symbols is given by

$$P_T = \mathrm{E}\left\{ \|\sum_{i=1}^{K} \mathbf{w}_i b_i\|^2 \right\} = \sum_{i=1}^{K} \|\mathbf{w}_i\|^2. \tag{5}$$

Note uthat the assumption of the symbols independence from SBS is not applied in our proposed approaches. In the following we present the two most common SINR-based CR downlink beamforming designs in the literature [5], [23], [24], which we will use as a reference for our proposed schemes. It is intuitive that the proposed concept can be applied to variations of these conventional beamforming problems.

A. Max-Min Fair Problem

The conventional SINR balancing CR downlink beamforming problem aims to maximize the minimum SINR subject to average interference and total transmitted power constraints.

The problem can be written as [5], [23]

$$\max_{\mathbf{w}_i,\gamma} \gamma$$

$$\text{s.t.} \frac{|\mathbf{h}_i^T \mathbf{w}_i|^2}{\sum_{\substack{j=1 \\ j\neq i}}^{K} |\mathbf{h}_i^T \mathbf{w}_j|^2 + \sigma^2} \geq \gamma,\ i = 1, \ldots, K, \tag{6a}$$

$$\sum_{i=1}^{K} \|\mathbf{w}_i\|^2 \leq P_0, \sum_{i=1}^{K} |\mathbf{g}_l^T \mathbf{w}_i|^2 \leq \epsilon_l,\ l = 1, \ldots, L, \tag{6b}$$

where P_0 is the total transmitted power budget and ϵ_l is the maximum admitted interference power caused by the SBS at the lth PU. The authors in [5] offered the fundamental approach based on the conventional downlink beamforming technique [15], while the authors in [23] provided the most efficient implementation. Problem (6) is feasible if the interference and power constraints in (6b) have a non-zero feasible point. By rotating the phase of $\mathbf{h}_i^T \mathbf{w}_i$, it can be assumed w.l.o.g. that $\mathbf{h}_i^T \mathbf{w}_i$ is real-valued and the solution still satisfies the constraints in (6a). Problem (6) can be rewritten as [5], [23]

$$\begin{aligned} \max_{\mathbf{w}_i,\gamma} \quad & \gamma \\ \text{s.t.} \quad & \mathrm{Im}(\mathbf{h}_i^T \mathbf{w}_i) = 0,\ i = 1, \ldots, K, \\ & \left\| \begin{matrix} (\mathbf{I}_K \otimes \mathbf{h}_i^T)\mathbf{w} \\ \sigma \end{matrix} \right\| \leq \sqrt{1 + \frac{1}{\gamma}} \mathbf{h}_i^T \mathbf{w}_i,\ i = 1, \ldots, K, \\ & \|\mathbf{w}\| \leq \sqrt{P_0},\ \|\mathbf{C}_{K+l}\mathbf{w}\| \leq \sqrt{\epsilon_l},\ l = 1, \ldots, L, \end{aligned} \tag{7}$$

where $\otimes$ is a Kronecker product and $\mathbf{w}$ and $\mathbf{C}_{K+l}$ are $NK \times 1$ and $K \times NK$ such that

$$\mathbf{w} \triangleq (\mathbf{w}_1^T\ \mathbf{w}_2^T \ldots \mathbf{w}_K^T)^T, \tag{8}$$

$$\mathbf{C}_{K+l} \triangleq \mathrm{blkdiag}(\underbrace{\mathbf{g}_l^T, \mathbf{g}_l^T, \ldots \mathbf{g}_l^T}_{K \text{ times}}). \tag{9}$$

Problem (7) is a quasi-convex optimization problem and can be solved using the bisection method and sequential SOCP. Nevertheless, the above problem does not take instantaneous interference exploitation into account for the transmit data symbols as a part of the optimization problem for each transmission. Moreover, our results in the simulations show that as per the average interference constraints in (7), the instantaneous interference may violate the interference power constraints, and could therefore lead to outages for the PUs.

In the next section, we consider to design the CR downlink precoding problem by making use of the instantaneous transmit data symbols to exploit constructive interference within the secondary links and restrict the instantaneous interference created by the SBS within primary links.

III. WSUSEP-Based CR Downlink Precoding for Interference Exploitation

A. Constructive Interference Exploitation

In the conventional downlink beamforming problems [10]–[16], precoders are designed by mitigating the average mutiuser interference, in which suppressing interference requires some degrees of freedom. It has been established in [43] that given the instantaneous transmit data symbols and CSI at the transmitter, it is not necessarily required to completely suppress the interference; instead the precoders can be designed to constructively use the interfering signal to enhance the desired signal. With the aid of exploiting the instantaneous interference and adapting the precoders, the constructive interference can alter the received signals further into the correct detection region to improve the system performance. Inspired by this idea, we provide a systematic treatment of constructive interference as illustrated in Fig. 2(a), where the nominal PSK constellation point is represented by the black circle. According to [43], we say that the received signal y_i exploits the interference constructively if y_i falls within the correct detection region, which is the shaded area shown in Fig. 2(a). Let ψ_i in Fig. 2(a) denote the angle between the received signal y_i and the transmitted symbol b_i in the complex plane. According to (2), the angle ψ_i depends on the transmitted signal $\mathbf{x}$ and the noise n_i. Hence the angle ψ_i can be treated as a function of $\mathbf{x}$ and n_i, i.e.,

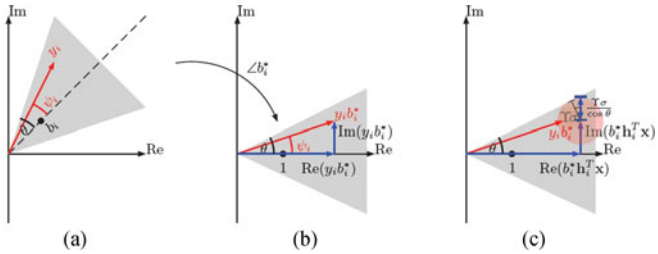

Fig. 2. For M-PSK modulation, (a) constructive interference y_i within correct detection region where the constructive area of constellation is indicted by the grey area; (b) after rotation by $\angle b_i^*$, $\mathrm{Re}(y_i b_i^*)$ and $\mathrm{Im}(y_i b_i^*)$ are projected from $y_i b_i^*$ on real and imaginary axis, respectively; (c) constructive interference is described using trigonometry.

$$\begin{aligned} \psi_i(\mathbf{x}, n_i) &= (\arg y_i - \arg b_i) \mod 2\pi \\ &= \arg(y_i b_i^*) = \tan^{-1}\left(\frac{\mathrm{Im}(y_i b_i^*)}{\mathrm{Re}(y_i b_i^*)}\right), \end{aligned} \tag{10}$$

where $\mathrm{Im}(y_i b_i^*)$ and $\mathrm{Re}(y_i b_i^*)$ are the projections of $y_i b_i^*$ onto the real and imaginary axis, respectively. The product $y_i b_i^*$ is displayed in Fig. 2(b) along with the corresponding decision region and the angle $\psi_i(\mathbf{x}, n_i)$. The received signal y_i of the i-th user is detected correctly, if and only if

$$\psi_i(\mathbf{x}, n_i) \in \mathcal{A}_{-\theta}^{\theta}, \qquad i = 1, \ldots, K, \tag{11}$$

where the angular set

$$\mathcal{A}_{\theta_1}^{\theta_2} \triangleq \left\{\tilde{\psi} \mod 2\pi \mid \theta_1 \leq \tilde{\psi} \leq \theta_2, \tilde{\psi} \in \mathbb{R}\right\}, \tag{12}$$

defines the decision region and $\theta = \pi/M$ is the maximum angular shift for an M-PSK constellation. Detailed deviations of the constructive interference regions for generic PSK modulations can be found in [43] and references therein. Based on above definition and discussion, we formulate in the following section the CR precoder design to exploit the instantaneous interference.

B. WSUSEP Approach

In this section, we derive the WSUSEP-based CR downlink precoding problem.[1] The idea of this approach is to design the precoders to steer the receive signals of SUs into the corresponding decision regions to reduce the corresponding symbol error. Furthermore, since the distribution of noise is known, we can calculate the symbol error probability (SEP) for each SU and use the WSUSEP as an objective function. The precoder design minimizes the WSUSEP subject to the instantaneous total transmit power and instantaneous interference power constraints, which can be written as

$$\min_{\mathbf{x},\rho} \quad \rho$$

$$\text{s.t.} \quad \Pr\big(\psi_i(\mathbf{x}, n_i) \in \mathcal{A}_{\theta}^{2\pi-\theta}\big) \le \rho,\ i = 1, \ldots, K, \quad (13a)$$

$$\|\mathbf{x}\|^2 \le P, |\mathbf{g}_l^T \mathbf{x}|^2 \le \epsilon_l,\ l = 1, \ldots, L, \quad (13b)$$

where ρ models the WSUSEP, $\Pr(\psi_i(\mathbf{x}, n_i) \in \mathcal{A}_{\theta}^{2\pi-\theta})$ is ith SU's SEP, i.e., the probability that the received signal falls outside the correct detection region and $\psi_i(\mathbf{x}, n_i) \notin \mathcal{A}_{-\theta}^{\theta}$, $\|\mathbf{x}\|^2$ is the instantaneous total transmitted power from the SBS, and $|\mathbf{g}_l^T \mathbf{x}|^2$ is the instantaneous interference power for SBS to the lth PU. We remark that the symbol synchronization is not required among the PBS and SBS systems. Firstly, the PBS does not need to know the existent of the SBS as it is up to the SBS to design the precoders such that the interference to PBS is less the predefined threshold. Secondly, the SBS does not need to synchronize with PBS. It only needs to know the channel $\mathbf{g}_l$ to the PUs, in order to constrain the interference to the primary link as per the interference temperature ϵ_l. This can be seen, for example, in (13b), where the SBS transmit symbol $\mathbf{x}$ need only align to $\mathbf{g}_l$ (and not the PBS transmit symbols) such that interference is constrained, and therefore no symbol-by-symbol synchronization is required; rather the primary link CSI requirement which is typical for this line of research as shown in the conventional formulation in (6b). Further note that the instantaneous interference power constraint in (13b) can be generalized to covariance-based interference power constraint without changing our formulation to reduce the CSI training feedback from PBS. For extending the covariance-based approach, please refer to [24] for more details. By considering the complement of the symbol error set, (13a) can be reformulated as

$$1 - \Pr\big(\psi_i(\mathbf{x}, n_i) \in \mathcal{A}_{-\theta}^{\theta}\big) \le \rho. \quad (14)$$

First let us simplify the set $\mathcal{A}_{-\theta}^{\theta}$ in (14), i.e., (11). By (10), the classification criteria (11) can be directly reformulated as the following alternatives

$$\text{I}: \ \frac{|\operatorname{Im}(y_i b_i^*)|}{\operatorname{Re}(y_i b_i^*)} \le \tan\theta, \quad \text{for } \operatorname{Re}(y_i b_i^*) > 0, \quad (15a)$$

$$\text{II}: \quad y_i b_i^* = 0, \quad \text{for } \operatorname{Re}(y_i b_i^*) = 0, \quad (15b)$$

which is equivalent to the single inequality

$$|\operatorname{Im}(y_i b_i^*)| - \operatorname{Re}(y_i b_i^*) \tan\theta \le 0. \quad (16)$$

[1]In this paper, we do not consider the power minimization problem as the power minimization solutions can be derived by the corresponding solutions to the WSUSEP optimization.

In this paper, we only consider M-PSK modulation schemes with $M \ge 4$.[2] Introducing the real-valued parameter vector representation

$$\bar{\mathbf{x}} \triangleq [\operatorname{Re}(\mathbf{x})^T,\ \operatorname{Im}(\mathbf{x})^T]^T, \quad (17)$$

$$\bar{\mathbf{h}}_i \triangleq [\operatorname{Im}(b_i^* \mathbf{h}_i)^T,\ \operatorname{Re}(b_i^* \mathbf{h}_i)^T]^T, \quad (18)$$

we can express the real and imaginary part of the transmitted signal in (16) as follows

$$\operatorname{Re}(b_i^* \mathbf{h}_i^T \mathbf{x}) = \bar{\mathbf{h}}_i^T \mathbf{\Pi}_K \bar{\mathbf{x}}, \quad (19)$$

$$\operatorname{Im}(b_i^* \mathbf{h}_i^T \mathbf{x}) = \bar{\mathbf{h}}_i^T \bar{\mathbf{x}}, \quad (20)$$

where $\mathbf{\Pi}_K \triangleq [\mathbf{0}_{K,K} \ -\mathbf{I}_K; \mathbf{I}_K \ \mathbf{0}_{K,K}]$ is a selection matrix. Resolving the absolute value term in (16), we obtain two linear inequalities

$$\mathbf{t}_{2i-1}^T \bar{\mathbf{x}} \ge \tilde{n}_{2i-1}, \quad (21a)$$

$$\mathbf{t}_{2i}^T \bar{\mathbf{x}} \ \ge \tilde{n}_{2i}, \quad (21b)$$

where

$$\mathbf{t}_{2i-1}^T \triangleq -\bar{\mathbf{h}}_i^T + \tan\theta\, \bar{\mathbf{h}}_i^T \mathbf{\Pi}_K, \quad (22)$$

$$\mathbf{t}_{2i}^T \ \triangleq \bar{\mathbf{h}}_i^T + \tan\theta\, \bar{\mathbf{h}}_i^T \mathbf{\Pi}_K, \quad (23)$$

$$\tilde{n}_{2i-1} \triangleq \operatorname{Im}(b_i^* n_i) - \operatorname{Re}(b_i^* n_i) \tan\theta, \quad (24)$$

$$\tilde{n}_{2i} \ \triangleq -\operatorname{Im}(b_i^* n_i) - \operatorname{Re}(b_i^* n_i) \tan\theta. \quad (25)$$

The vectors $\mathbf{t}_j,\ j = 1, \ldots, 2K$, are deterministic and depend on the channel and the decision region defined by the angle θ, and the scalars $\tilde{n}_j$ are real-valued Gaussian random variables (linear transformations of Gaussian random variables). By (21), the probability function in (14) can be written as a joint probability function

$$\Pr\Big(\mathbf{t}_{2i-1}^T \bar{\mathbf{x}} \ge \tilde{n}_{2i-1}, \mathbf{t}_{2i}^T \bar{\mathbf{x}} \ge \tilde{n}_{2i}\Big). \quad (26)$$

Consider the bivariate standard normal probability distribution ϕ with zero mean such that

$$\phi(\mathbf{u}; r) = \frac{1}{2\pi\sqrt{1-r^2}} \exp\left(-\frac{1}{2}\mathbf{u}^T \mathbf{\Sigma}^{-1} \mathbf{u}\right), \quad (27)$$

where $\mathbf{u} \triangleq [u_1,\ u_2]^T$, the correlation r is defined as

$$r \triangleq \frac{\mathrm{E}\{\eta_1 \eta_2\}}{\sqrt{\mathrm{E}\{|\eta_1|^2\}\mathrm{E}\{|\eta_2|^2\}}} = \mathrm{E}\{\eta_1 \eta_2\}, \quad (28)$$

with $|r| < 1$, η_1, η_2 are the standardized random variables, i.e., $\mathrm{E}\{|\eta_1|^2\} = \mathrm{E}\{|\eta_2|^2\} = 1$, and

$$\mathbf{\Sigma} \triangleq \mathrm{E}\big\{[\eta_1, \eta_2]^T [\eta_1, \eta_2]\big\} = \begin{bmatrix} 1 & r \\ r & 1 \end{bmatrix}. \quad (29)$$

The cumulative distribution function (CDF) of the standard bivariate normal distribution is defined by

$$\Phi(\mathbf{u}; r) = \int_{-\infty}^{u_1} \int_{-\infty}^{u_2} \phi(\tilde{\mathbf{u}}; r)\, d\tilde{u}_1 d\tilde{u}_2. \quad (30)$$

[2]Note that $\tan\theta = \infty$ for $M = 2$ as $\theta = \pi/2$. In this case, the constraint in (14) can be formulated as $1 - \Pr(\operatorname{Re}(y_i b_i^*) \ge 0) \le \rho$, which can reformulated using the univariate normal cumulative distribution function. The corresponding optimization in (13) is convex when $\rho^\star \le 0.5$ where $\rho^\star$ is the optimal value of (35), i.e., $\operatorname{Re}(b_i^* \mathbf{h}_i^T \mathbf{x}) \ge 0$.

Then the corresponding probability function for $u_1 \geq \eta_1, u_2 \geq \eta_2$ is given by

$$\Pr\Big(u_1 \geq \eta_1, u_2 \geq \eta_2\Big) = \Phi(\mathbf{u}; r). \tag{31}$$

Since n_i in (2) is a circularly symmetric zero mean complex Gaussian random variable, we can conclude that $\tilde{n}_j$ in (24) and (25) is also a real-valued Gaussian with zero mean and variance

$$\sigma_{\tilde{n}}^2 \triangleq \mathrm{E}\{\tilde{n}_j^2\} = \frac{(1+\tan^2\theta)\sigma^2}{2} = \frac{\sigma^2}{2\cos^2\theta}, \tag{32}$$

i.e., $\tilde{n}_j \sim \mathcal{N}(0, \frac{\sigma^2}{2\cos\theta^2})$. Since $\tilde{n}_{2i-1}$and $\tilde{n}_{2i}$ correspond to a real bivariate normal distribution and according to (31), we can express (26) as a joint normal CDF

$$\Phi\left(\left[\frac{\mathbf{t}_{2i-1}^T\bar{\mathbf{x}}}{\sigma_{\tilde{n}}}, \frac{\mathbf{t}_{2i}^T\bar{\mathbf{x}}}{\sigma_{\tilde{n}}}\right]^T; \bar{r}\right), \tag{33}$$

with the correlation of $\tilde{n}_{2i-1}$ and $\tilde{n}_{2i}$ is given by

$$\bar{r} = \frac{-1+\tan^2\theta}{1+\tan^2\theta} = -\cos 2\theta. \tag{34}$$

By (14) and (33), problem (13) can be reformulated as

$$\min_{\mathbf{x},\rho} \quad \rho$$

$$\text{s.t.} \quad 1 - \Phi\left(\left[\frac{\mathbf{t}_{2i-1}^T\bar{\mathbf{x}}}{\sigma_{\tilde{n}}}, \frac{\mathbf{t}_{2i}^T\bar{\mathbf{x}}}{\sigma_{\tilde{n}}}\right]^T; \bar{r}\right) - \rho \leq 0, \ i = 1, \ldots, K, \tag{35a}$$

$$\|\bar{\mathbf{x}}\| - \sqrt{P} \leq 0, \|\mathbf{B}_l\bar{\mathbf{x}}\| - \sqrt{\epsilon_l} \leq 0, \ l = 1, \ldots, L, \tag{35b}$$

where

$$\mathbf{B}_l \triangleq \begin{bmatrix} \mathrm{Re}(\mathbf{g}_l^T) & -\mathrm{Im}(\mathbf{g}_l^T) \\ \mathrm{Im}(\mathbf{g}_l^T) & \mathrm{Re}(\mathbf{g}_l^T) \end{bmatrix} \tag{36}$$

is a $2 \times 2N$ real matrix. We remark that constraint (35a) is generally non-convex. Note that the sufficient condition for the concavity of the standard bivariate normal CDF is non-trivial. Author in [26] showed that $\Phi(\mathbf{u}; r)$ is concave in one variable under a certain condition on u_1 and u_2, respectively.

Lemma 1A: [26] (Concavity in one variable - positive correlation) Let $r \geq 0$. Then $\Phi(\mathbf{u}; r)$ is concave in u_i for fixed u_j with $j \neq i$, i.e., $\frac{\partial^2\Phi(\mathbf{u};r)}{\partial u_i^2} \leq 0$ for $i = 1, 2$.

Lemma 1B: [26] (Concavity in one variable - negative correlation) Let $-1 \leq r \leq 0$. Then $\Phi(\mathbf{u}; r)$ is concave in u_i for fixed u_j with $j \neq i$, i.e., $\frac{\partial^2\Phi(\mathbf{u};r)}{\partial u_i^2} \leq 0$ for $i = 1, 2$, if

$$u_i \geq \sqrt{\frac{\phi(1)}{2\Phi(1)+\phi(1)}}, \ i = 1, 2, \tag{37}$$

where the probability density function and CDF of a standard univariate normal distribution are given by

$$\phi(u) = \frac{1}{\sqrt{2\pi}}\exp\left(-\frac{u^2}{2}\right), \Phi(u) = \int_{-\infty}^{u}\phi(\tilde{u})\,d\tilde{u}, \tag{38}$$

respectively.

In this paper, we further restrict the conditions on variables to guarantee the joint concavity of the CDF in (35a) and show that these conditions are generally met in conventional transmission scenarios.

Theorem 1: (Joint Concavity) For $M \geq 4$, the standard bivariate normal CDF in (35a) is concave if $\mathbf{t}_j^T\bar{\mathbf{x}}$ satisfies the inequality

$$\mathbf{t}_j^T\bar{\mathbf{x}}/\sigma_{\tilde{n}} \geq \alpha^\star(\bar{r}), \ j = 1, \ldots, 2K, \tag{39}$$

with threshold $\alpha^\star(\cdot)$ denoting the optimal function value of the following constrained optimization problem:

$$\alpha^\star(r): \min_{\alpha} \ \alpha \ \text{s.t.} \ \frac{\Phi\left(\alpha\frac{1-r}{\sqrt{1-r^2}}\right)}{\phi\left(\alpha\frac{1-r}{\sqrt{1-r^2}}\right)}\alpha \geq \frac{1-r}{\sqrt{1-r^2}}. \tag{40}$$

Proof: See Appendix A. ■

Following from (35a), we have

$$\Phi\left(\left[\frac{\mathbf{t}_{2i-1}^T\bar{\mathbf{x}}}{\sigma_{\tilde{n}}}, \frac{\mathbf{t}_{2i}^T\bar{\mathbf{x}}}{\sigma_{\tilde{n}}}\right]^T; \bar{r}\right) \geq 1 - \rho \geq 1 - \rho^\star, \tag{41}$$

where $\rho^\star$ is the optimal value of (35). Moreover, by the definition of univariate and bivariate normal CDFs and with $\Phi(\mathbf{u}; r)$ being an increasing function on r for fixed $\mathbf{u}$, we obtain

$$\begin{aligned}\Phi\left(\frac{\mathbf{t}_j^T\bar{\mathbf{x}}}{\sigma_{\tilde{n}}}\right) &= \int_{-\infty}^{\infty}\int_{-\infty}^{\frac{\mathbf{t}_j^T\bar{\mathbf{x}}}{\sigma_{\tilde{n}}}}\phi(\tilde{\mathbf{u}}; 0)\,d\tilde{u}_1 d\tilde{u}_2 \\ &\geq \Phi\left(\left[\frac{\mathbf{t}_{2i-1}^T\bar{\mathbf{x}}}{\sigma_{\tilde{n}}}, \frac{\mathbf{t}_{2i}^T\bar{\mathbf{x}}}{\sigma_{\tilde{n}}}\right]^T; 0\right) \\ &\geq \Phi\left(\left[\frac{\mathbf{t}_{2i-1}^T\bar{\mathbf{x}}}{\sigma_{\tilde{n}}}, \frac{\mathbf{t}_{2i}^T\bar{\mathbf{x}}}{\sigma_{\tilde{n}}}\right]^T; \bar{r}\right),\end{aligned} \tag{42}$$

for $j = 2i-1, 2i$. Hence, this yields

$$\Phi\left(\frac{\mathbf{t}_j^T\bar{\mathbf{x}}}{\sigma_{\tilde{n}}}\right) \geq 1 - \rho^\star, \tag{43}$$

for $j = 1, \ldots, 2K$. If we assume that

$$1 - \rho^\star \geq \Phi(\alpha^\star(\bar{r})), \tag{44}$$

then, by inequalities (43)-(44), and the strict monotonicity property of the standard univariate normal CDF, we ensure that condition (39) is satisfied. Thus, by Theorem 1, the assumption in (44) can guarantee problem (35) to be convex. That is, as of Theorem 1, for the optimal value $\rho^\star$ of (35) such that $1 - \Phi(\alpha^\star(\bar{r})) \geq \rho^\star$ for a given correlation $\bar{r}$, the optimization problem in (35) is convex. In Table I, we list, as examples, the lower bounds of (39) and the upper bounds of $\rho^\star$ for different values M of the constellation size. For example, when $M = 4$, the value of $\rho^\star$ in (44) corresponds to a SEP of less than 30.64% which does not put any restrictions on our precoder design as in typical applications much lower SEP values are required. Accordingly, the optimization problem in (35) is convex for all practical SEP constraints.

Suppose the conditions in (39) of Theorem 1 are satisfied, then (35) can be written as a convex optiminization problem and can be solved by any contemporary methods such as the subgradient projection and barrier methods [49]. For the sake of

TABLE I
THE CORRELATION $\bar{r}$, LOWER BOUNDS OF (39) AND UPPER BOUNDS OF THE OPTIMAL VALUE $\rho^\star$ OF (35) FOR DIFFERENT CONSTELLATION SIZE M

M	$\bar{r}$	$\alpha^\star(\bar{r})$	$1-\Phi(\alpha^\star(\bar{r}))$
4	0	0.5061	0.3064
8	−0.7071	0.5088	0.3055
16	−0.9239	0.3694	0.3559
32	−0.9808	0.2353	0.4070
64	−0.9952	0.1400	0.4443

illustration, we choose to use the barrier method to solve (35). Let

$$\Psi(\bar{\mathbf{x}},\rho) \triangleq -\sum_{i=1}^{K}\ln\left(-\left(1-\Phi\left(\left[\frac{\mathbf{t}_{2i-1}^T\bar{\mathbf{x}}}{\sigma_{\tilde{n}}},\ \frac{\mathbf{t}_{2i}^T\bar{\mathbf{x}}}{\sigma_{\tilde{n}}}\right]^T;\bar{r}\right)-\rho\right)\right) - \ln(-(\|\bar{\mathbf{x}}\|-\sqrt{P})) - \sum_{i=1}^{K}\ln(-(\|\mathbf{B}_l\bar{\mathbf{x}}\|-\sqrt{\epsilon_l})), \tag{45}$$

be the logarithmic barrier function. For $s>0$, define $\bar{\mathbf{x}}(s)$ and $\rho(s)$ as the solution of

$$\min_{\bar{\mathbf{x}},\rho}\ \rho+\Psi(\bar{\mathbf{x}},\rho)/s. \tag{46}$$

Problem (46) is an unconstrained convex optimization problem and can be solved using the gradient descent algorithm [49]. Problem (35) is feasible if the constraints in (35a)-(35b) contain a non-zero feasible point. In particular, a feasible starting point of the barrier method can be computed as the solution of the following feasibility problem

$$\max_{\bar{\mathbf{x}},z}\ z \text{ s.t. } z\ \le \mathbf{t}_j^T\bar{\mathbf{x}},\ j=1,\ldots,2K, \quad \|\bar{\mathbf{x}}\|\ \le\sqrt{P},\ \|\mathbf{B}_l\bar{\mathbf{x}}\|\le\sqrt{\epsilon_l},\ l=1,\ldots,L, \tag{47}$$

which is a SOCP problem that can be solved efficiently. Suppose $(z^\star,\bar{\mathbf{x}}^\star(1))$ is an optimal point of (47). The first observation is that if the assumption in (44) is satisfied, then $z^\star\ge\sigma_{\tilde{n}_j}\alpha^\star(\bar{r})$ is also satisfied. Reversely, if $z^\star<\sigma_{\tilde{n}_j}\alpha^\star(\bar{r})$, then the assumption in (44) is not true. In this case the problem is ill-posed as the SEP of the SUs exceed the values that are reasonable in practical applications. If $z^\star\ge\sigma_{\tilde{n}_j}\alpha^\star(\bar{r})$, then, by Theorem 1, problem (35) is a convex problem and (47) provides us a feasible starting point of the barrier method.

Algorithm 1 summarizes the steps to compute the solution of (35) using barrier method. For more details on the barrier method, the reader is referred to [49, p.561-p.613]. We observe in the simulations that Algorithm 1 provides a better performance compared to the conventional approach in [5], [23].

Remark 3: The optimal precoding vectors $\mathbf{w}_i^\star, i=1,\ldots,K$ corresponding to the solutions of (13) can be computed using (1) as

$$\mathbf{w}_i^\star=\frac{\mathbf{x}^\star b_i^*}{K}, \tag{48}$$

where $\mathbf{x}^\star$ is the optimal solution in (13).

Algorithm 1: Efficient barrier method to solve (35).

Given: $s=1,\mu>1$, tolerance $\delta_t>0$
Input: $\{\mathbf{h}_i\}_{i=1}^K,\{b_i\}_{i=1}^K,P_0,\sigma,\bar{r}$
Output: The optimal solution $(\bar{\mathbf{x}}^\star,\rho^\star)$ of (35)
Determine the optimal solution $(z^\star,\bar{\mathbf{x}}^\star(1))$ of (47);
If $z^\star<\sigma_{\tilde{n}_j}\alpha^\star(\bar{r})$, then no practical solution was found;
Set

$$\rho^\star(1)=\min_{1\le i\le K}\{1-\Phi(\tilde{\mathbf{t}}_i(\bar{\mathbf{x}}^\star(1));\bar{r})\};$$

repeat
  Compute the optimal solution $(\bar{\mathbf{x}}^\star(s),\rho^\star(s))$ of (46);
  Set $s=\mu s$;
until $\|\bar{\mathbf{x}}^\star(s)-\bar{\mathbf{x}}^\star(s-1)\|^2+|\rho^\star(s)-\rho^\star(s-1)|^2<\delta_t^2$;
Output $\bar{\mathbf{x}}^\star(s),\rho^\star(s)$;

IV. COMPUTATIONALLY EFFICIENT APPROXIMATE APPROACH

A. Computationally Efficient Approximate WSUSEP Minimization Problem

In this section, we aim to provide a low complexity approximate approach to the WSUSEP-based CR downlink precoding problem in (13) that achieves a tight approximation. Considering the addition law of probability, the left-hand side of (13a) can be expressed as

$$\Pr\big(\psi_i\in\mathcal{A}_\theta^{2\pi-\theta}\big)=\Pr\big(\psi_i\in\mathcal{A}_\theta^{\pi+\theta}\big)+\Pr\big(\psi_i\in\mathcal{A}_{\pi-\theta}^{2\pi-\theta}\big)-\Pr\big(\psi_i\in\mathcal{A}_{\pi-\theta}^{\pi+\theta}\big), \tag{49}$$

where

$$\Pr\big(\psi_i\in\mathcal{A}_\theta^{\pi+\theta}\big)=\Pr\big(\psi_i\in\mathcal{A}_\theta^{\frac{\pi}{2}}\vee\mathcal{A}_{\frac{\pi}{2}}^{\pi+\theta}\big)=\Pr\big(\tilde{n}_{2i-1}\ge\mathbf{t}_{2i-1}^T\bar{\mathbf{x}}\big), \tag{50}$$

$$\Pr\big(\psi_i\in\mathcal{A}_{\pi-\theta}^{2\pi-\theta}\big)=\Pr\big(\psi_i\in\mathcal{A}_{\pi-\theta}^{\frac{3\pi}{2}}\vee\mathcal{A}_{\frac{3\pi}{2}}^{2\pi-\theta}\big)=\Pr\big(\tilde{n}_{2i}\ge\mathbf{t}_{2i}^T\bar{\mathbf{x}}\big), \tag{51}$$

are the probabilities that ψ_i take values in the left and right half plane of Fig. 2(b), respectively, i.e., between θ and $\pi+\theta$ and between $\pi-\theta$ and $2\pi-\theta$, respectively, $\vee$ is the logical "OR" operator, $\Pr\big(\mathcal{A}_{\pi-\theta}^{\pi+\theta}\big)$ is the probability of ψ_i taking a value in the intersection of the left and right half planes given above. We remark that the precoders are designed to steer the received signals into the corresponding corrected detection regions and hence generally $\Pr\big(\psi_i\in\mathcal{A}_{\pi-\theta}^{\pi+\theta}\big)$ takes small values. Therefore, by (49), (50) and (51), we can approximate (13a) as

$$\Pr\big(\psi_i\in\mathcal{A}_\theta^{2\pi-\theta}\big)\le\Pr\Big(\tilde{n}_{2i-1}\ge\mathbf{t}_{2i-1}^T\bar{\mathbf{x}}\Big)+\Pr\Big(\tilde{n}_{2i}\ge\mathbf{t}_{2i}^T\bar{\mathbf{x}}\Big)\le\rho. \tag{52}$$

Further restricting (52) by the following two constraints

$$\Pr\Big(\tilde{n}_{2i-1} \geq \mathbf{t}_{2i-1}^T \bar{\mathbf{x}}\Big) \leq \rho/2,\ \Pr\Big(\tilde{n}_{2i} \geq \mathbf{t}_{2i}^T \bar{\mathbf{x}}\Big) \leq \rho/2, \quad (53)$$

the optimization problem in (13) can be approximately written as

$$\begin{aligned} \min_{\mathbf{x},\rho}\ & \rho \\ \text{s.t. }\ & \Pr\Big(\tilde{n}_{2i-1} \geq \mathbf{t}_{2i-1}^T \bar{\mathbf{x}}\Big) \leq \rho/2,,\ i = 1,\ldots,K, && \text{(54a)} \\ & \Pr\Big(\tilde{n}_{2i} \geq \mathbf{t}_{2i}^T \bar{\mathbf{x}}\Big) \leq \rho/2,\ i = 1,\ldots,K, && \text{(54b)} \\ & \|\mathbf{x}\|^2 \leq P, |\mathbf{g}_l^T \mathbf{x}|^2 \leq \epsilon_l,\ l = 1,\ldots,L, && \text{(54c)} \end{aligned}$$

which is the worst-case design on $\Pr(\tilde{n}_j \geq \mathbf{t}_j^T \bar{\mathbf{x}})$ for $j = 1,\ldots,2K$. The approximate problem (54) represents a restriction of problem (13) as in the sense that any optimal point of (54) is feasible for (13), but the reverse statement is generally not true. This means that (54) is an inner approximation to (13). Based on (32), we have [25]

$$\Pr\Big(\tilde{n}_j \geq \mathbf{t}_j^T \bar{\mathbf{x}}\Big) = \int_{\mathbf{t}_j^T \bar{\mathbf{x}}}^{\infty} \frac{\cos\theta}{\sqrt{\pi}\sigma} e^{\frac{\tilde{n}^2 \cos^2\theta}{\sigma^2}} d\tilde{n}. \quad (55)$$

Using the Gaussian error function $\mathrm{erf}(\cdot)$, the SEP in (55) can be expressed as [25]

$$\Pr\Big(\tilde{n}_j \geq \mathbf{t}_j^T \bar{\mathbf{x}}\Big) = \begin{cases} \frac{1}{2} + \frac{1}{2}\,\mathrm{erf}\Big(\frac{-\mathbf{t}_j^T \bar{\mathbf{x}} \cos\theta}{\sigma}\Big), & \mathbf{t}_j^T \bar{\mathbf{x}} \leq 0, \\ \frac{1}{2} - \frac{1}{2}\,\mathrm{erf}\Big(\frac{\mathbf{t}_j^T \bar{\mathbf{x}} \cos\theta}{\sigma}\Big), & \mathbf{t}_j^T \bar{\mathbf{x}} \geq 0. \end{cases} \quad (56)$$

Since $\mathrm{erf}(-x) = -\mathrm{erf}(x)$, we rewrite (56) as

$$\frac{1}{2} - \frac{1}{2}\,\mathrm{erf}\left(\frac{\mathbf{t}_j^T \bar{\mathbf{x}} \cos\theta}{\sigma}\right) \leq \rho/2, \quad (57)$$

which is equivalent to

$$\frac{\sigma\,\mathrm{erf}^{-1}(1-\rho)}{\cos\theta} \leq\ \mathbf{t}_j^T \bar{\mathbf{x}}, \quad (58)$$

where $\mathrm{erf}^{-1}(\cdot)$ is the inverse error function. The approximate problem (54) can be written as a function $\rho^\star(\cdot)$ for any given transmit power $P \geq 0$ such that

$$\begin{aligned} \rho^\star(P): \min_{\bar{\mathbf{x}},\rho}\ & \rho \\ \text{s.t. }\ & -\mathbf{t}_j^T \bar{\mathbf{x}} + \frac{\sigma\,\mathrm{erf}^{-1}(1-\rho)}{\cos\theta}\mathbf{1}_{2K} \leq 0, \\ & j = 1,\ldots,2K, \\ & \|\bar{\mathbf{x}}\| \leq \sqrt{P}, \|\mathbf{B}_l \bar{\mathbf{x}}\| \leq \sqrt{\epsilon_l},\ l = 1,\ldots,L. && \text{(59)} \end{aligned}$$

As the inverse error function $\mathrm{erf}^{-1}(v)$ is monotonously increasing in the interval $-1 < v < 1$, we can equivalently write (59) as the following problem

$$\begin{aligned} \max_{\bar{\mathbf{x}},\Upsilon}\ & \Upsilon\sigma \\ \text{s.t. }\ & -\mathbf{t}_j^T \bar{\mathbf{x}} + \frac{\Upsilon\sigma}{\cos\theta}\mathbf{1}_{2K} \leq 0,\ j = 1,\ldots,2K, && \text{(60a)} \\ & \|\bar{\mathbf{x}}\| \leq \sqrt{P}, \|\mathbf{B}_l \bar{\mathbf{x}}\| \leq \sqrt{\epsilon_l},\ l = 1,\ldots,L, && \text{(60b)} \end{aligned}$$

where $\Upsilon = \mathrm{erf}^{-1}(1-\rho)$ is a scalar optimization variable and $\Upsilon^\star(\tilde{P})$ is the optimal value of Υ in (63) for a given transmit power $\tilde{P}$. Due to the monotonicity property of error function and inverse error function, there exists a one-to-one mapping from Υ to ρ, and vice versa. Then we obtain the following relations:

$$\Upsilon^\star(P) = \ \mathrm{erf}^{-1}(1-\rho^\star(P)), \quad (61)$$

$$\rho^\star(P) = \ \frac{1}{2} - \frac{1}{2}\,\mathrm{erf}(\Upsilon^\star(P)), \quad (62)$$

$$\bar{\mathbf{x}}_\rho^\star(P) = \ \bar{\mathbf{x}}_\Upsilon^\star(P), \quad (63)$$

and $\bar{\mathbf{x}}_\rho^\star(\tilde{P})$ and $\bar{\mathbf{x}}_\Upsilon^\star(\tilde{P})$ are optimal solutions of (59) and (60) for a given power $\tilde{P}$, respectively. Problem (60) is SOCP and can be solved efficiently using convex optimization tools such as CVX [50]. The optimal precoding vectors $\mathbf{w}_i^\star, i = 1,\ldots,K$ corresponding to the solutions of (54) can be computed using (1) as

$$\mathbf{w}_i^\star = \frac{\mathbf{x}^\star b_i^*}{K}, \quad (64)$$

where $\mathbf{x}^\star$ is the optimal solution in (54).

B. Computational Complexity

1) Transmit Complexity: Here we provide a transmit complexity comparison for the conventional and proposed approximate approaches, for the slow fading channel (respectively, fast fading channel). The conventional SINR balancing CR downlink beamforming problem (7) is a sequential SOCP problem. The single SOCP in (7) can be solved with a worst-case complexity of $\mathcal{O}(N^3K^3(K+L)^{1.5})$ using efficient barrier methods [51]. The number of SOCP iterations is bounded above by $\mathcal{O}(\log I)$ where $I\delta_t$ is the range of the search space for γ in (7) and δ_t is the error tolerance. As the optimization problem in (7) is data independent, it only needs to be applied once per frame (respectively, sub-frame) for the slow fading case (respectively, fast fading case). The complexity C_{CA} per downlink frame (respectively, sub-frame) for the conventional CR approach is of the order

$$C_{CA} \sim \mathcal{O}(N^3(K+L)^{1.5}K^3 \log I). \quad (65)$$

The proposed approximate approach (54) is a SOCP problem, which requires a worst-case complexity of $\mathcal{O}(N^3(K+L)^{1.5})$. As the proposed optimization problem in (54) is data dependent, the number N_{SOCP} of SOCP compuations per frame for slow fading (respectively, the channel coherence sub-frame for fast fading) is equal to the number of data time-slots in the frame (respectively, sub-frame). Accordingly, the resulting complexity C_{PAA} per downlink frame (respectively, sub-frame) for the proposed approximate approach is of the order

$$C_{PAA} \sim \mathcal{O}(N^3(K+L)^{1.5}N_{\mathrm{SOCP}}). \quad (66)$$

Therefore, if $\mathcal{O}(K^3 \log I)$ and $\mathcal{O}(N_{\mathrm{SOCP}})$ are comparable, then it can be seen from (65)-(66) that the worst-case complexities of the proposed approximate and conventional CR downlink beamforming problems are also comparable. In the following simulations, using typical LTE Type 2 TDD frame scheme [52], we show that the average execution time per downlink frames

for the proposed approximate approach in (54) is comparable to that of conventional CR beamforming for both slow and fast fading scenarios.

2) Receiver Complexity: It should be noted at this point that, compared to conventional beamforming, the proposed approaches provide significant complexity benefits at the receiver side. Indeed, as the received symbols lie at the constructive area of the constellation (see Fig. 2), there is no need for equalizing the composite channel $\mathbf{h}_i^T \mathbf{w}_i^c$ to recover the data symbols at the ith SU, where $\{\mathbf{w}_i^c\}_{i=1}^K$ is the optimal solution of (7). Accordingly, this straightforwardly translates to complexity savings at the SUs compared to conventional approaches. Furthermore, for the proposed approaches this entails that CSI is not required for detection at the SU. Hence, depending on the signalling and pilots already involved for SINR estimation, the proposed approaches may further lead to savings in the training time and overhead for the signalling the precoders for SUs. We note that some of the existing standards already employ precoded pilots for SINR estimation [53], so the above operation would not add any particular overhead. Nevertheless, the above feature of the proposed schemes can lead to significant reductions in the operation time, and more importantly makes the proposed precoders immune to any quantization errors in the relevant signalling.

C. Geometric Interpretation

Problem (60) can be interpreted as the problem of placing the centers of K largest balls with centers $(\mathrm{Re}(b_i^* \mathbf{h}_i^T \mathbf{x}), \mathrm{Im}(b_i^* \mathbf{h}_i^T \mathbf{x}))$, $(i = 1, \ldots, K)$ and with maximum radii $\Upsilon\sigma$ inside the decision region. This can then be interpreted as designing the SU precoding vectors such that under a given power constraint the detection procedure applied to the received signal becomes most immune to noise as can be observed from Fig. 2(c). The precoder design maximizes the radius $\Upsilon\sigma$ of the noise uncertainty set (i.e., $|n_i| \leq \Upsilon\sigma$) within the correct detection region. As we can see from Fig. 2(c), when the radius $\Upsilon\sigma$ of the noise uncertainty set is larger, the chance of the receive symbol falling outside the decision region reduce. As illustrated in Fig. 2(c), by ensuring the correct detection region containing the noise uncertainty set, we have the following inequalities

$$\frac{|\mathrm{Im}(b_i^* \mathbf{h}_i^T \mathbf{x})| + \Upsilon\sigma/\cos\theta}{\mathrm{Re}(b_i^* \mathbf{h}_i^T \mathbf{x})} \leq \tan\theta, \quad \text{for } \mathrm{Re}(b_i^* \mathbf{h}_i^T \mathbf{x}) > 0, \tag{67a}$$

$$\Upsilon = 0, \qquad \text{for } b_i^* \mathbf{h}_i^T \mathbf{x} = 0, \tag{67b}$$

which are equivalent to the constraint in (60a). Therefore the proposed WSUSEP in (13) in its tight approximation in (60) can also be interpreted as the following worst-users received symbol center placement problem:

$$\begin{aligned} \max_{\mathbf{x},\Upsilon} \ & \Upsilon\sigma \\ \text{s.t.} \ & \max_{|n_i| \leq \Upsilon\sigma} |\psi_i(\mathbf{x}, n_i)| \leq \theta, \ i = 1, \ldots, K, \\ & \|\mathbf{x}\|^2 \leq P, \ |\mathbf{g}_l^T \mathbf{x}| \leq \sqrt{\epsilon_l}, \ l = 1, \ldots, L. \end{aligned} \tag{68}$$

V. Simulations

In this section, we present simulation results for a constructive interference-based downlink precoding for CR network with $N = 10$ antennas and $L = 2$ PU. Note that the benefits shown extend to different numbers of antennas. The system with M-PSK modulation is considered, i.e., $\theta = \pi/M$. With respect to the above setup, we note that in practical applications adaptive coded modulation (ACM) would be employed to adapt to any variations in the average received SNR. Here, however, following the closely related literature we focus our comparisons to specific modulations and transmit power levels that allow to observe the performance trend under reasonable error rate performance down to an uncoded worst user symbol error rate (WUSER) of $10^{-3} - 10^{-4}$ for the channel model employed, for both the conventional and proposed techniques. Clearly, the benefits of our proposed techniques extend to power levels, SNRs, channel models and noise variances other than the ones employed in the following. Furthermore, the observed benefits extend to higher order modulations as demonstrated for our particular scenario here by representative results in the following. Following the setup in our benchmark schemes, channel vectors $\mathbf{h}_i$ are normalized to unit power, and a noise variance value of $\sigma^2 = 0.1$ is considered, while it is intuitive that the benefits of the proposed approach extend to other values. In line with [54], we assume that the SUs and PUs connected to the SBS are located at directions

$$\begin{aligned} \omega_{1,\ldots,10} &= \left[3^\circ, 35^\circ, 10^\circ, 39^\circ, 17^\circ, 74^\circ, 24^\circ, 86^\circ, 30^\circ, 80^\circ\right]^T + \mathbf{r}_1, \\ \tilde{\omega}_{1,2} &= \ [50^\circ, 57^\circ]^T + \mathbf{r}_2, \end{aligned} \tag{69}$$

where $\mathbf{r}_1 \in \mathbb{C}^{10}$ and $\mathbf{r}_2 \in \mathbb{C}^2$ are drawn from a uniform distribution in the interval $[-1^\circ, 1^\circ]$. Then the downlink channel from the SBS to ith SU and lth PU are modeled as [54]

$$\mathbf{h}_i = \left[1, e^{j\pi \sin\omega_i}, \ldots, e^{j\pi(N-1)\sin\omega_i}\right]^T, \tag{70}$$

$$\mathbf{g}_l = \left[1, e^{j\pi \sin\tilde{\omega}_l}, \ldots, e^{j\pi(N-1)\sin\tilde{\omega}_l}\right]^T. \tag{71}$$

We note that, with the above channel model the power of the channel vectors is normalised to 1. According to (10), we use the angle ψ_i between the received signal y_i and the transmitted symbol b_i as an measure of the correct detection, which evaluates the performance of our proposed methods and the conventional method of (7). The receive signal can be correctly detected if ψ_i is within the interval $[-\theta, \theta]$. We introduce the normalized constraint value of interference power on an instantaneous basis [24]

$$\zeta_l = \frac{\sum_{j=1}^K \sum_{i=1}^K b_j^* b_i \mathbf{w}_j^{\star H} \mathbf{g}_l^* \mathbf{g}_l^T \mathbf{w}_i^\star}{\epsilon_l}, \tag{72}$$

as an abstract measure of the constraint satisfaction to compare the performance of different methods. The corresponding instantaneous interference power constraint at PU is satisfied if and only if $\zeta_l \leq 1$. All results are average over 10^6 Monte Carlo runs. The average execution time is defined to be the average running time for calculating the optimization problems for a given scenario, where the CSI estimation is not included, on the

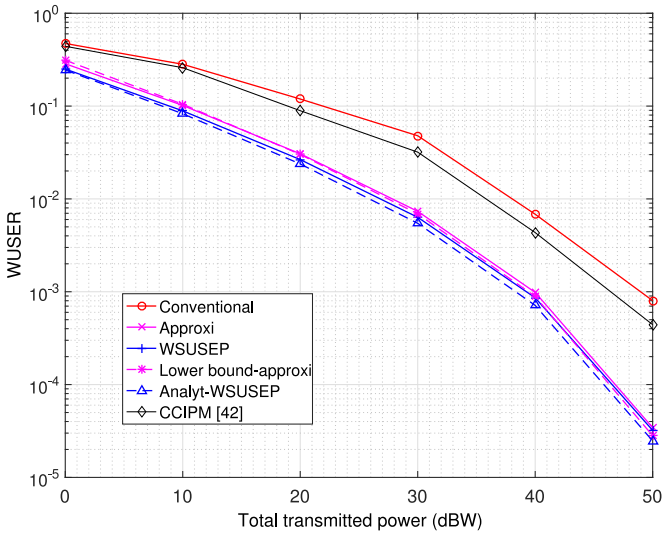

Fig. 3. WUSER performance versus power with $N = 10$, $L = 2$, $K = 8$, $\epsilon_l = -2$ dBW, and QPSK modulation.

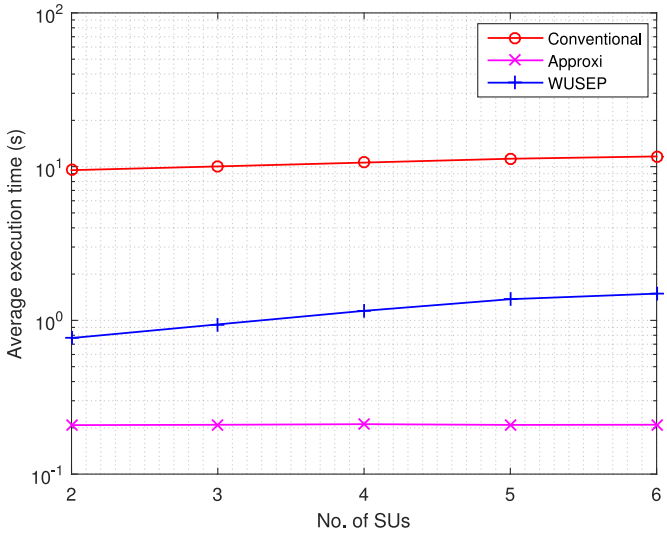

Fig. 4. Average execution time per optimization versus number of SUs with $N = 10$, $L = 2$, $P = 50$ dBW, $\epsilon_l = -2$ dBW, and QPSK modulation.

Intel Dual Core i5 4210U CPU 4.00GB RAM laptop with 1.7 and 2.4 GHz.

In the following simulations, we compare three different techniques:

1) 'Conventional' refers to the max-min fair problem (7) in [5], [23];
2) 'Approxi' stands for the computationally efficient approximation of the WSUSEP-based optimization given in (59);
3) 'WSUSEP' refers to the WSUSEP-based approach given in (35);
4) 'CCIPM [42]' stands for the CR symbol based precoding in [45], translated to the Z-channel scenario here;

and 'Analyt-WSUSEP' and 'Lower bound-approxi' stand for $\mathrm{mean}(\{\rho_i^\star\})$ and $\mathrm{mean}(\{\tilde{\rho}_i^\star\})$, respectively, where $\rho_i^\star$ and $\tilde{\rho}_i^\star$ are the optimal values of (35) and (59) for ith Monte Carlo run, respectively, and $\mathrm{mean}(\cdot)$ is the average function.

In Fig. 3, we fix the number of SUs and compare the WUSER performance of our proposed approaches and the conventional approach of (7) versus the total transmitted power P for $K = 8$, $\epsilon_l = -2$ dBW, and QPSK modulation. It can be seen from Fig. 3 that the proposed approaches given in (35) and (59) outperform the conventional method of (7) and the symbol based precoding in [45] in terms of the experimental WUSER performances. Notably, it can be observed in Fig. 3 that our analytic WUSER performance and lower bound of the computationally efficient approximate approach calculations match the experimental WUSER results of both (35) and (59), respectively. Furthermore, the computationally efficient approximate approach calculations match closely to the WSUSEP approach. Note that in the simulations, we assume that in conventional approach the ith user receives the composite channel $\mathbf{h}_i^T \mathbf{w}_i^c$ from the SBS without any errors, which requires to decode the symbol b_i. However, the estimation of the composite channel $\mathbf{h}_i^T \mathbf{w}_i^c$ and feedback procedure to SU may result in estimation errors or reconstruction losses introduced by CSI quantization, which is required due to resource limitations of the feedback channels. The erroneous composite channel may further deteriorate the performances in Fig. 3 for the conventional approach.

Fig. 4 compares the trend of the average execution time per optimization of our proposed methods and the conventional method for different number of SUs with $P = 50$ dBW, $\epsilon_l = -2$ dBW, and QPSK modulation. As shown in Fig. 4, when the number of SUs increase, the average execution time per optimization of the conventional method is much slower than the WSUSEP method and the computationally efficient approximate approach. Furthermore, we can see from the figure, the computationally efficient approximate approach is indifferent from the number of SUs. Note that we adopt the LTE Type 2 TDD frame scheme in [52]. Within a frame, 5 sub-frames, in which contains 14 symbols per each time-slot, are used for downlink (DL) transmission. Therefore, for the DL, it yields a block size of $B = 70$. A slow fading channel is assumed to be constant for the duration of one frame. In Fig. 5, we show the average execution time per DL frame for different number of SUs in slow fading channel scenario based on Fig. 4. Although the end complexity is higher for our proposed method compared to the conventional method, the constructive interference based precoding problem is still worthwhile as it improves the WUSER of SUs and secure the QoS of PUs on an instantaneous basis. For fast fading channel, we assumed the channel to be constant for the duration of one sub-frame [52], which means that the channel changes 5 times per frame. Fig. 5 also depicts the average execution time per DL sub-frame for different number of SUs in fast fading channel scenario based on Fig. 4. For this case, it can seen that our proposed approach offers a significant reduction in execution time down to around 30%.

In Figs. 6–8, we fix the transmitted power and vary the number of SUs, the size of PSK modulations, and the maximum allowable interference powers, respectively. Fig. 6 displays (both the experimental and analytic) WUSER performance for

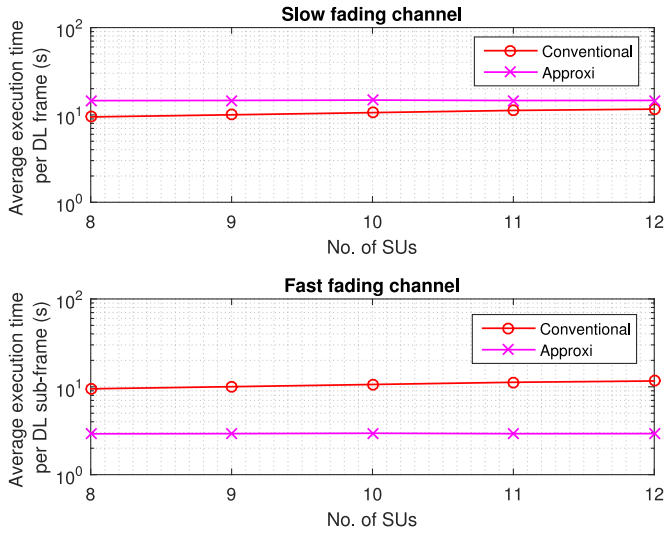

Fig. 5. Average execution time versus number of SUs for slow/fast fading channels with $N = 10$, $L = 2$, $P = 50\,\text{dBW}$, $\epsilon_l = -2\,\text{dBW}$, and QPSK modulation.

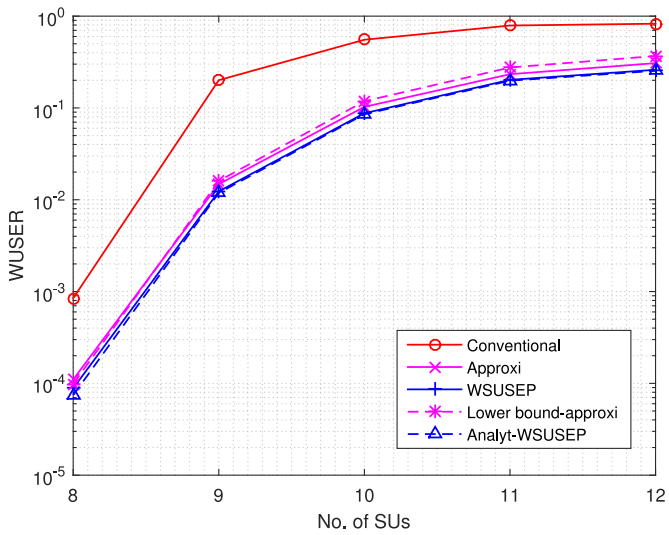

Fig. 6. WUSER versus number of SUs with $N = 10$, $L = 2$, $P = 50\,\text{dBW}$, $\epsilon_l = -2\,\text{dBW}$, and QPSK modulation.

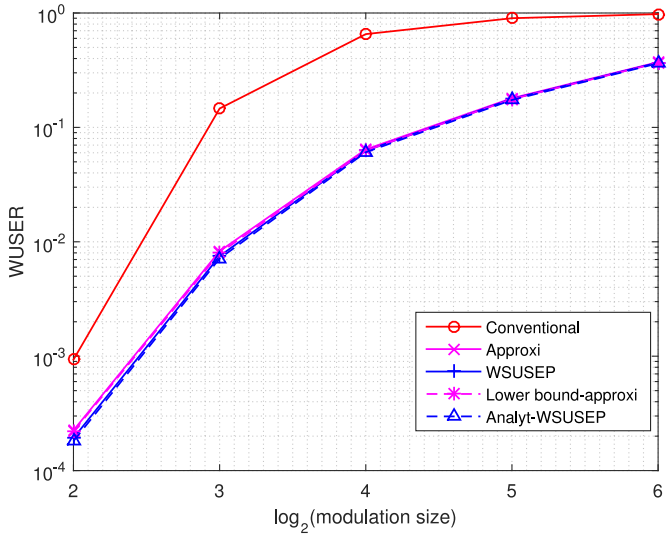

Fig. 7. WUSER performance versus log of modulation size with $N = 10$, $L = 2$, $K = 8$, $\epsilon_l = -2\,\text{dBW}$, and $P = 50\,\text{dBW}$.

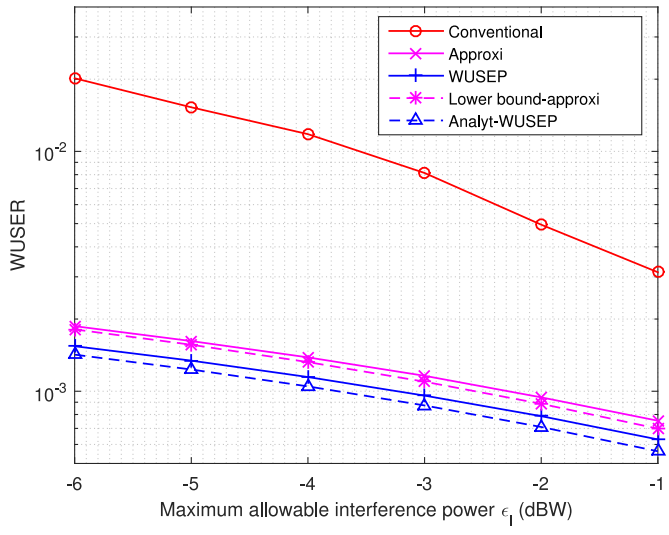

Fig. 8. WUSER performance versus maximum allowable interference power ϵ_l with $N = 10$, $L = 2$, $K = 8$, $P = 40\,\text{dBW}$, and QPSK modulation.

various number of SUs when we set the modulation to be QPSK with $\epsilon_l = -2\,\text{dBW}$ and $P = 50\,\text{dBW}$. We observe that the experimental SER performance of our proposed approaches are better than the conventional approach. The computationally efficient approximate approach is a good approximation method for the WSUSEP approach. In Fig. 7, we compare the performance versus different size of PSK modulations for the different techniques with $K = 8$, $\epsilon_l = -2\,\text{dBW}$ and $P = 50\,\text{dBW}$. As can be seen from the figure, the proposed methods outperform the conventional method especially when the size of modulations is small. Fig. 8 depicts the WUSER performance versus different maximum allowable interference powers ϵ_l with $K = 8$, $P = 40\,\text{dBW}$, and QPSK modulation. We see from Fig. 8 that our proposed methods perform better than the conventional method.

In Figs. 9–11, we look at the distribution of the decoded signals and instantaneous interference power, respectively. Fig. 9 depicts the distribution of the decoded signals using different techniques on complex plane with $K = 8$, $\epsilon_l = -2\,\text{dBW}$, and $P = 5\,\text{dBW}$, and QPSK modulation. For the purposes of illustration, we show the example for which $b_i = 1$ for $i = 1, \ldots, N$. Then we can see that the right side of dotted line is the correct detection region. In particular, the decoded signal is valid if it lays on the right side behind the dotted line. We observe from Fig. 9 that the decoded signals of our proposed methods can better fall into the correct detection region compared to the conventional method. Fig. 10 displays the histograms of the angles ψ_i between the received signal y_i and the transmitted symbol b_i with $K = 8$, $\epsilon_l = -2\,\text{dBW}$, $P = 5\,\text{dBW}$, and QPSK modulation. The angles outside the interval $[-\pi/4, \pi/4]$ are counted as errors. The first observation is that all approaches have normal-

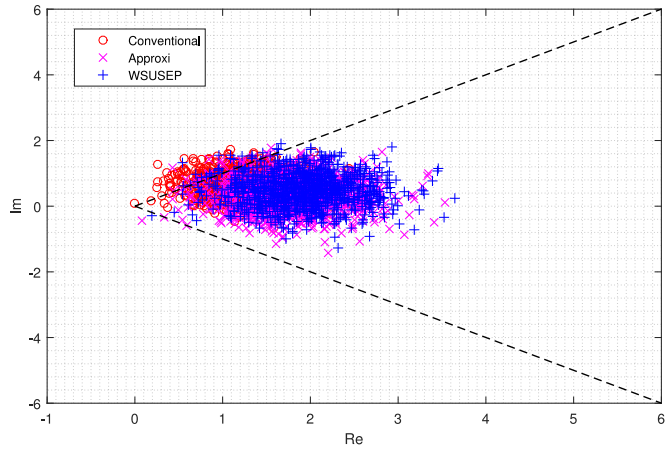

Fig. 9. Distribution of decoded signals on complex plane where $N = 10$, $L = 2$, $K = 8$, $\epsilon_l = -2$ dBW, $P = 5$ dBW, and QPSK modulation.

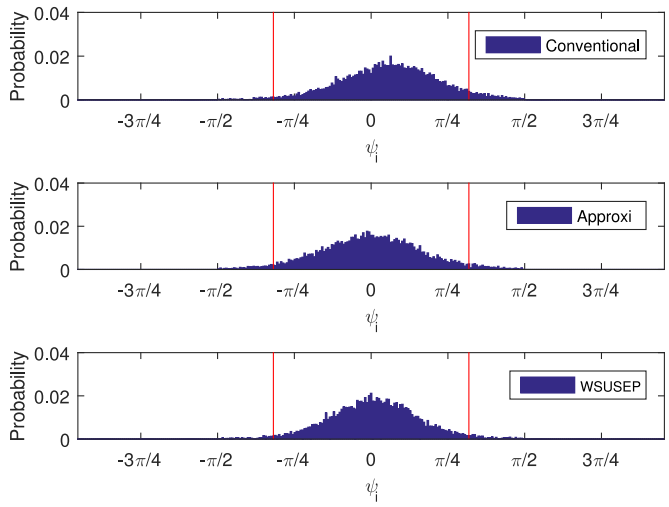

Fig. 10. Histogram of the angles ψ_i with $N = 10$, $L = 2$, $K = 8$, $\epsilon_l = -2$ dBW, $P = 5$ dBW, and QPSK modulation.

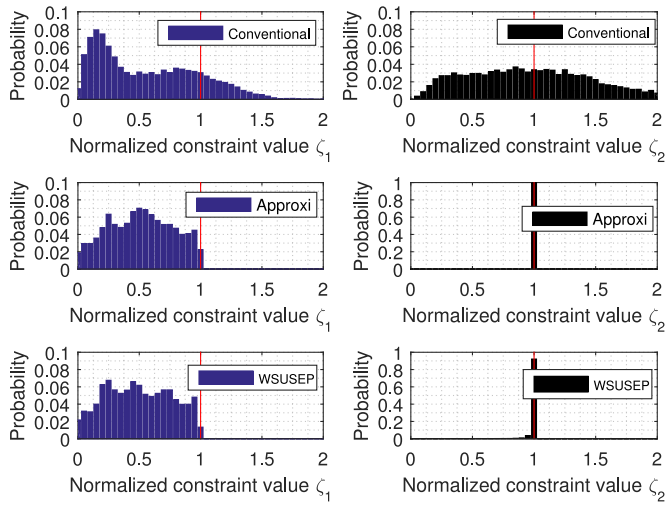

Fig. 11. Histogram of normalized constraint values ζ_l with $N = 10$, $L = 2$, $K = 8$, $\epsilon_l = -2$ dBW, $P = 5$ dBW, and QPSK modulation.

like distributions. As can be observed from Fig. 10, it is more likely that the received symbol falls outside the desired region for the conventional method compared to the proposed methods. Fig. 11 depicts the histograms of normalized constraint values ζ_l given in (72) with $K = 8$, $\epsilon_l = -2$ dBW, $P = 5$ dBW, and QPSK modulation. As can be observed from Fig. 11, the conventional technique only satisfies about 50% of the instantaneous interference power constraints for the second PU. This is due to the fact that the conventional method only considers the average interference power. However, our proposed approaches always satisfy the interference power constraints on an instantaneous basis. This consists of significant improvement over conventional CR beamformers which are prone to instantaneous SINR violations which could cause PU outages.

VI. Conclusion

In this paper, we exploit the constructive interference in the underlay CR Z-channel by making use of CSI and transmit data information jointly. Our approach minimizes the WSUSEP of the SUs, subject to SBS transmit power constraints, while guaranteeing the PUs' QoS on an instantaneous basis. The proposed optimization can be formulated as a the bivariate probabilistic constrained programming problem. Under a condition on SEP, the problem can be expressed as a convex optimization problem and can be solved efficiently. We also propose a computationally efficient approximate approach to the WSUSEP approach to reduce the complexity. Simulation results have shown that our proposed methods have significantly improved performance as compared to the conventional CR downlink beamforming method. Future work can focus on extending our proposed constructive interference-based approaches by considering the robustness to CSI errors.

Appendix

A. Proof of Theorem 1

To show the concavity, we need to use the first and second derivatives. It is well-known that taking the first derivative with respect to u_1, we have [26]

$$\frac{\partial \Phi(\mathbf{u}; r)}{\partial u_1} = \Phi(u_2|u_1)\phi(u_1), \tag{73}$$

where the conditional distribution function $\Phi(u_2|u_1)$ is described by

$$\Phi(u_2|u_1) = \Phi\Big(\frac{u_2 - ru_1}{\sqrt{1-r^2}}\Big). \tag{74}$$

Similarly, we have $\frac{\partial \Phi(\mathbf{u};r)}{\partial u_2} = \Phi(u_1|u_2)\phi(u_2)$. Taking the second mixed derivative, we have

$$\frac{\partial^2 \Phi(\mathbf{u}; r)}{\partial u_1 \partial u_2} = \phi\left(\frac{u_2 - ru_1}{\sqrt{1-r^2}}\right)\frac{1}{\sqrt{1-r^2}}\phi(u_1) \tag{75}$$

$$= \phi\left(\frac{u_1 - ru_2}{\sqrt{1-r^2}}\right)\frac{1}{\sqrt{1-r^2}}\phi(u_2). \tag{76}$$

Taking the second derivative with respect to u_1, we have

$$\frac{\partial^2\Phi(\mathbf{u};r)}{\partial u_1^2} = \left(\phi\left(\frac{u_2-ru_1}{\sqrt{1-r^2}}\right)\frac{-r}{\sqrt{1-r^2}} - u_1\Phi\left(\frac{u_2-ru_1}{\sqrt{1-r^2}}\right)\right)\phi(u_1)$$
$$= -r\frac{\partial^2\Phi(\mathbf{u};r)}{\partial u_1\partial u_2} - u_1\frac{\partial\Phi(\mathbf{u};r)}{\partial u_1}. \quad (77)$$

Similarly, we have $\frac{\partial^2\Phi(\mathbf{u};r)}{\partial u_2^2} = -r\frac{\partial^2\Phi(\mathbf{u};r)}{\partial u_1\partial u_2} - u_2\frac{\partial\Phi(\mathbf{u};r)}{\partial u_2}$.

By an abuse of notation, we redefine $\tilde{n}_j = \tilde{n}_j/\sigma_{\tilde{n}_j}$ and define $t_j(\bar{\mathbf{x}}) \triangleq \mathbf{t}_j^T\bar{\mathbf{x}}/\sigma_{\tilde{n}_j}$. Then $\tilde{n}_j$ is a standardized random variable for all j. To show the standard bivariate normal CDF in (35a) is concave, it is enough to prove that the Hessian matrix of the CDF

$$\left[\begin{array}{cc}\frac{\partial t_{2i-1}}{\partial\bar{\mathbf{x}}}^T & \frac{\partial t_{2i}}{\partial\bar{\mathbf{x}}}^T\end{array}\right]\mathbf{M}_i\left[\begin{array}{cc}\frac{\partial t_{2i-1}}{\partial\bar{\mathbf{x}}}^T & \frac{\partial t_{2i}}{\partial\bar{\mathbf{x}}}^T\end{array}\right]^T, \quad (78)$$

is a negative-semidefinite matrix where

$$\mathbf{M}_i \triangleq \left[\begin{array}{cc}\frac{\partial^2\Phi}{\partial t_{2i-1}^2} & \frac{\partial^2\Phi}{\partial t_{2i-1}\partial t_{2i}} \\ \frac{\partial^2\Phi}{\partial t_{2i-1}\partial t_{2i}} & \frac{\partial^2\Phi}{\partial t_{2i}^2}\end{array}\right]. \quad (79)$$

The matrix in (78) is negative-semidefinite if the eigenvalues $\lambda_i^{\pm}$ of $\mathbf{M}_i$ are negative, which are equal to

$$\lambda_i^{\pm} = \frac{\left(\frac{\partial^2\Phi}{\partial t_{2i-1}^2} + \frac{\partial^2\Phi}{\partial t_{2i}^2}\right) \pm \sqrt{\Delta_i}}{2}, \quad (80)$$

where $\Delta_i \triangleq (\frac{\partial^2\Phi}{\partial t_{2i-1}^2} - \frac{\partial^2\Phi}{\partial t_{2i}^2})^2 + 4(\frac{\partial^2\Phi}{\partial t_{2i-1}\partial t_{2i}})^2$. First the eigenvalues are real values as $\Delta_i \geq 0$. Second, by (34), we have $-1 \leq \bar{r} \leq 0$, for $M \geq 4$. Then, by (39) and Lemma 1B, we have

$$\frac{\partial^2\Phi}{\partial t_j^2} \leq 0, \quad (81)$$

which implies that $(\frac{\partial^2\Phi}{\partial t_{2i-1}^2} + \frac{\partial^2\Phi}{\partial t_{2i}^2}) \leq 0$. In order to show both eigenvalues are negative, we need to show that

$$-\left(\frac{\partial^2\Phi}{\partial t_{2i-1}^2} + \frac{\partial^2\Phi}{\partial t_{2i}^2}\right) \geq \sqrt{\Delta_i}, \quad (82)$$

which is equivalent to

$$\frac{\partial^2\Phi}{\partial t_{2i-1}^2}\frac{\partial^2\Phi}{\partial t_{2i}^2} \geq \left(\frac{\partial^2\Phi}{\partial t_{2i-1}\partial t_{2i}}\right)^2. \quad (83)$$

If

$$-\frac{\partial^2\Phi}{\partial t_{2i-1}^2} \geq \frac{\partial^2\Phi}{\partial t_{2i-1}\partial t_{2i}}, \; -\frac{\partial^2\Phi}{\partial t_{2i}^2} \geq \frac{\partial^2\Phi}{\partial t_{2i-1}\partial t_{2i}}, \quad (84)$$

then (83) holds. The inequalities in (84) can be rewritten as

$$\frac{\Phi\left(\frac{t_{2i}-\bar{r}t_{2i-1}}{\sqrt{1-\bar{r}^2}}\right)}{\phi\left(\frac{t_{2i}-\bar{r}t_{2i-1}}{\sqrt{1-\bar{r}^2}}\right)}t_{2i-1} \geq \frac{1-\bar{r}}{\sqrt{1-\bar{r}^2}}, \quad (85)$$

$$\frac{\Phi\left(\frac{t_{2i-1}-\bar{r}t_{2i}}{\sqrt{1-\bar{r}^2}}\right)}{\phi\left(\frac{t_{2i-1}-\bar{r}t_{2i}}{\sqrt{1-\bar{r}^2}}\right)}t_{2i} \geq \frac{1-\bar{r}}{\sqrt{1-\bar{r}^2}}, \quad (86)$$

respectively. The inequalities in (85) and (86) are satisfied for $t_{2i-1} \geq \alpha$, $t_{2i} \geq \alpha$, if we have

$$\frac{\Phi\left(\alpha\frac{1-\bar{r}}{\sqrt{1-\bar{r}^2}}\right)}{\phi\left(\alpha\frac{1-\bar{r}}{\sqrt{1-\bar{r}^2}}\right)}\alpha \geq \frac{1-\bar{r}}{\sqrt{1-\bar{r}^2}}. \quad (87)$$

To find the minimum α, we can solve the optimization problem in (40). Hence, for $t_{2i-1} \geq \alpha^\star(\bar{r})$, $t_{2i} \geq \alpha^\star(\bar{r})$, the inequalities in (85) and (86) hold. This completes the proof of the theorem. ■

REFERENCES

[1] J. Mitola and G. Q. Maguire, "Cognitive radio: Making software radios more personal," *IEEE Pers. Commun.*, vol. 6, no. 4, pp. 13–18, Aug. 1999.

[2] S. Haykin, "Cognitive radio: Brain-empowered wireless communications," *IEEE J. Sel. Areas Commun.*, vol. 23, no. 2, pp. 201–220, Feb. 2005.

[3] Q. Zhao and B. M. Sadler, "A survey of dynamic spectrum access," *IEEE Signal Process. Mag.*, vol. 24, no. 3, pp. 79–89, May 2007.

[4] S. Sankaranarayanan, P. Papadimitratos, A. Mishra, and S. Hershey, "A bandwidth sharing approach to improve licensed spectrum utilization," in *Proc. 1st IEEE Int. Symp. New Frontiers Dyn. Spectr. Access Netw.*, Nov. 2005, pp. 279–288.

[5] R. Zhang, Y.-C. Liang, and S. Cui, "Dynamic resource allocation in cognitive radio networks," *IEEE Signal Process. Mag.*, vol. 27, no. 3, pp. 102–114, May 2010.

[6] L. Zhang, Y.-C. Liang, and Y. Xin, "Joint beamforming and power allocation for multiple access channels in cognitive radio networks," *IEEE J. Sel. Areas Commun.*, vol. 26, no. 1, pp. 38–51, Jan. 2008.

[7] H. Islam, Y.-C. Liang, and A. T. Hoang, "Joint beamforming and power control in the downlink of cognitive radio networks," in *Proc. IEEE Wireless Commun. Netw. Conf.*, Mar. 2007, pp. 21–26.

[8] E. Dahlman, S. Parkvall, and J. Skold, *4G: LTE/LTE-Advanced for Mobile Broadband: LTE/LTE-Advanced for Mobile Broadband*. Amsterdam, The Netherlands: Elsevier, 2011.

[9] A. F. Molisch, *Wireless Communications*. Hoboken, NJ, USA: Wiley, 2011.

[10] F. Rashid-Farrokhi, K. Liu, and L. Tassiulas, "Transmit beamforming and power control for cellular wireless systems," *IEEE J. Sel. Areas Commun.*, vol. 16, no. 8, pp. 1437–1450, Oct. 1998.

[11] M. Schubert and H. Boche, "Solution of the multiuser downlink beamforming problem with individual SINR constraints," *IEEE Trans. Veh. Technol.*, vol. 53, no. 1, pp. 18–28, Jan. 2004.

[12] M. Bengtsson and B. Ottersten, "Optimal downlink beamforming using semidefinite optimization," in *Proc. Annu. Allerton Conf. Commun. Control Comput.*, 1999, vol. 37, pp. 987–996.

[13] M. Bengtsson and B. Ottersten, "Optimal and suboptimal transmit beamforming," *Handbook of Antennas in Wireless Communications*. Boca Raton, FL, USA: CRC Press, 2001.

[14] A. Wiesel, Y. C. Eldar, and S. Shamai, "Linear precoding via conic optimization for fixed MIMO receivers," *IEEE Trans. Signal Process.*, vol. 54, no. 1, pp. 161–176, Jan. 2006.

[15] A. B. Gershman, N. D. Sidiropoulos, S. Shahbazpanahi, M. Bengtsson, and B. Ottersten, "Convex optimization-based beamforming: From receive to transmit and network designs," *IEEE Signal Process. Mag.*, vol. 27, no. 3, pp. 62–75, May 2010.

[16] J. Choi, "Downlink multiuser beamforming with compensation of channel reciprocity from RF impairments," *IEEE Trans. Commun.*, vol. 63, no. 6, pp. 2158–2169, Jun. 2015.

[17] M. Costa, "Writing on dirty paper," *IEEE Trans. Inf. Theory*, vol. 59, no. 1, pp. 439–441, May 1983.
[18] U. Erez, S. Shamai, and R. Zamir, "Capacity and lattice strategies for canceling known interference," *IEEE Trans. Inf. Theory*, vol. 51, no. 11, pp. 3820–3833, Nov. 2005.
[19] B. Hassibi and H. Vikalo, "On the expected complexity of integer least-squares problems," in *Proc. IEEE Int. Conf. Acoust. Speech, Signal Process.*, May 2002, vol. 2, pp. II-1497–II-1500.
[20] C. Windpassinger, R. F. H. Fischer, T. Vencel, and J. B. Huber, "Precoding in multiantenna and multiuser communications," *IEEE Trans. Wireless Commun.*, vol. 3, no. 4, pp. 1305–1316, Jul. 2004.
[21] C. Masouros, M. Sellathurai, and T. Ratnarajah, "Interference optimization for transmit power reduction in Tomlinson-Harashima precoded MIMO downlinks," *IEEE Trans. Signal Process.*, vol. 60, no. 5, pp. 2470–2481, May 2012.
[22] A. Garcia-Rodriguez and C. Masouros, "Power-efficient Tomlinson-Harashima precoding for the downlink of multi-user MISO systems," *IEEE Trans. Commun.*, vol. 62, no. 6, pp. 1884–1896, Jun. 2014.
[23] X. Fu, J. Wang, and S. Li, "Joint power management and beamforming for base stations in cognitive radio systems," in *Proc. 6th Int. Symp. Wireless Commun. Syst.*, Sep. 2009, pp. 403–407.
[24] I. Wajid, M. Pesavento, Y. Eldar, and D. Ciochina, "Robust downlink beamforming with partial channel state information for conventional and cognitive radio networks," *IEEE Trans. Signal Process.*, vol. 61, no. 14, pp. 3656–3670, Jul. 2013.
[25] B. Chalise, S. ShahbazPanahi, A. Czylwik, and A. Gershman, "Robust downlink beamforming based on outage probability specifications," *IEEE Trans. Wireless Commun.*, vol. 6, no. 10, pp. 3498–3503, Oct. 2007.
[26] A. Prékopa, "On probabilistic constrained programming," *Math. Program. Study*, vol. 28, pp. 113–138, 1970.
[27] C. Masouros and E. Alsusa, "Soft linear precoding for the downlink of DS/CDMA communication systems," *IEEE Trans. Veh. Technol.*, vol. 59, no. 1, pp. 203–215, Jan. 2010.
[28] E. Alsusa and C. Masouros, "Interference exploitation using adaptive code allocation for the downlink of precoded mc-cdma systems," *IEEE Trans. Wireless Commun.*, vol. 8, no. 7, pp. 3634–3645, Jul. 209.
[29] C. Masouros and E. Alsusa, "Dynamic linear precoding for the exploitation of known interference in MIMO broadcast systems," *IEEE Trans. Wireless Commun.*, vol. 8, no. 3, pp. 1396–1404, Mar. 2009.
[30] C. Masouros, "Correlation rotation linear precoding for MIMO broadcast communications," *IEEE Trans. Signal Process.*, vol. 59, no. 1, pp. 252–262, Jan. 2011.
[31] A. Li and C. Masouros, "Exploiting constructive mutual coupling in p2p mimo by analog-digital phase alignment," *IEEE Trans. Wireless Commun.*, vol. 15, no. 3, pp. 1948–1962, Mar. 2017.
[32] P. V. Amadori and C. Masouros, "Constant envelope precoding by interference exploitation in phase shift keying-modulated multiuser transmission," *IEEE Trans. Wireless Commun.*, vol. 16, no. 1, pp. 539–550, Jan. 2017.
[33] P. V. Amadori and C. Masouros, "Interference driven antenna selection for massive multi-user mimo," *IEEE Trans. Veh. Technol.*, vol. 65, no. 5, pp. 3139–3149, Aug. 2016.
[34] C. Masouros, T. Ratnarajah, M. Sellathurai, C. Papadias, and A. Shukla, "Known interference in the cellular downlink: A performance limiting factor or a source of green signal power?" *IEEE Commun. Mag.*, vol. 51, no. 10, pp. 162–171, Oct. 2013.
[35] G. Zheng, I. Krikidis, C. Masouros, S. Timotheou, D.-A. Toumpakaris, and Z. Ding, "Rethinking the role of interference in wireless networks," *IEEE Commun. Mag.*, vol. 52, no. 11, pp. 152–158, Nov. 2014.
[36] M. Alodeh, S. Chatzinotas, and B. Ottersten, "Energy-efficient symbol-level precoding in multiuser MISO based on relaxed detection region," *IEEE Trans. Wireless Commun.*, vol. 15, no. 5, pp. 3755–3767, May 2016.
[37] M. Alodeh, S. Chatzinotas, and B. Otterste, "Constructive multiuser interference in symbol level precoding for the MISO downlink channel," *IEEE Trans. Signal Process.*, vol. 63, no. 9, pp. 2239–2252, May 2015.
[38] M. P. Daly and J. T. Bernhard, "Directional modulation technique for phased arrays," *IEEE Trans. Antennas Propag.*, vol. 57, no. 9, pp. 2633–2640, Sep. 2009.
[39] T. Hong, M. Z. Song, and Y. Liu, "Dual-beam directional modulation technique for physical-layer secure communication," *IEEE Antennas Wireless Propag. Lett.*, vol. 10, pp. 1417–1420, Dec. 2011.
[40] Y. Ding and V. F. Fusco, "A vector approach for the analysis and synthesis of directional modulation transmitters," *IEEE Trans. Antennas Propag.*, vol. 62, no. 1, pp. 361–370, Jan. 2014.
[41] A. Kalantari, M. Soltanalian, S. Maleki, S. Chatzinotas, and B. Ottersten, "Secure M-PSK communication via directional modulation," in *Proc. IEEE Int. Conf. Acoust., Speech, Signal Process.*, Mar. 2016, pp. 3481–3485.
[42] A. Kalantari, M. Soltanalian, S. Maleki, S. Chatzinotas, and B. Ottersten, "Directional modulation via symbol-level precoding: A way to enhance security," *IEEE J. Sel. Topics Signal Process.*, vol. 10, no. 8, pp. 1478–1493, Dec. 2016.
[43] C. Masouros and G. Zheng, "Exploiting known interference as green signal power for downlink beamforming optimization," *IEEE Trans. Signal Process.*, vol. 63, no. 14, pp. 3628–3640, Jul. 2015.
[44] K. L. Law, C. Masouros, K.-K. Wong, and G. Zheng, "Constructive interference exploitation for QoS-based downlink beamforming optimization," *IEEE Trans. Wireless Commun.*, in press.
[45] M. Alodeh, S. Chatzinotas, and B. Ottersten, "Symbol based precoding in the downlink of cognitive MISO channel," in *Proc. 10th Int. Conf., Doha, Qatar*, Apr. 2015, pp. 21–23.
[46] G. S. Smith, "A direct derivation of a single-antenna reciprocity relation for the time domain," *IEEE Trans. Antennas Propag.*, vol. 52, no. 6, pp. 1568–1577, Jun. 2004.
[47] S. Vishwanath, N. Jindal, and A. Goldsmith, "The "Z" channel," in *Proc. IEEE Glob. Telecommun. Conf.*, Dec. 2003, vol. 3, pp. 1726–1730.
[48] M. Alodeh, S. Chatzinotas, and B. Ottersten, "Constructive interference through symbol level precoding for multi-level modulation," in *Proc. IEEE Glob. Commun. Conf.*, Dec. 2015, pp. 1–6.
[49] S. Boyd and L. Vandenberghe, *Convex Optimization*. Cambridge, U.K.: Cambridge Univ. Press, 2004.
[50] *CVX: Matlab Software for Disciplined Convex Programming,* Version 2.1, CVX Res., Inc., San Ramon, CA, USA, Jun. 2015.
[51] M. S. Lobo, L. Vandenberghe, S. Boyd, and H. Lebret, "Applications of second-order cone programming," *Linear Algebra Appl.*, vol. 284, pp. 4193–228, Sep. 1998.
[52] 3GPP, "Evolved Universal Terrestrial Radio Access (E-UTRA); LTE Physical Layer; General Description," 3GPP, Sophia Antipolis, France, TS 36.201, V11.1.0 (2008–03), Release 11, 2008.
[53] N. J. M. Kobayashi and G. Caire, "Training and feedback optimization for multiuser mimo downlink," *IEEE Trans. Commun.*, vol. 59, no. 8, pp. 2228–2240, Aug. 2011.
[54] Y. Huang and D. Palomar, "Rank-constrained separable semidefinite programming with applications to optimal beamforming," *IEEE Trans. Signal Process.*, vol. 58, no. 2, pp. 664–678, Feb. 2010.

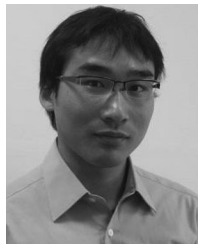

Ka Lung Law (S'09) was born in Hong Kong, in 1979. He received the B.Sc. degree major in computer science from the University of Melbourne, Melbourne, Vic, Australia, in 2002, the B.Sc. degree in mathematics from the University of Illinois at Urbana-Champaign, Champaign, IL, USA, in 2003, and the Ph.D. degree in mathematics with computational science and engineering option from the Department of Mathematics, University of Illinois at Urbana-Champaign, in 2008. From 2009, he was with the Department of Communication Systems, Technische Universität, Darmstadt, Germany. In 2016, he was a Research Associate in the Department of Electronics and Electrical Engineering, University College London. He is currently a Senior Algorithmic Engineer at Huawei Technologies Co. Ltd., Shenzen, China.

Christos Masouros (M'06–SM'14) received the Diploma degree in electrical and computer engineering from the University of Patras, Patras, Greece, in 2004, and the M.Sc. degree by research and Ph.D. degree in electrical and electronic engineering from the University of Manchester, Manchester, U.K., in 2006 and 2009, respectively. In 2008, he was a Research Intern at Philips Research Labs, U.K. Between 2009 and 2010, he was a Research Associate with the University of Manchester and between 2010 and 2012 a Research Fellow in Queen's University Belfast. He has held a Royal Academy of Engineering Research Fellowship between 2011 and 2016.

He is currently a Senior Lecturer in the Communications and Information Systems research group, Department of Electrical and Electronic Engineering, University College London, London, U.K. His research interests include the field of wireless communications and signal processing with particular focus on green communications, large-scale antenna systems, cognitive radio, interference mitigation techniques for MIMO and multicarrier communications. He received the Best Paper Award in the IEEE GlobeCom 2015 conference, and has been recognized as an Exemplary Editor for the IEEE COMMUNICATIONS LETTERS, and as an Exemplary Reviewer for the IEEE TRANSACTIONS ON COMMUNICATIONS. He is an Editor for IEEE TRANSACTIONS ON COMMUNICATIONS, an Associate Editor for IEEE COMMUNICATIONS LETTERS, and was a Guest Editor for IEEE JOURNAL ON SELECTED TOPICS IN SIGNAL PROCESSING issue "Exploiting Interference towards Energy Efficient and Secure Wireless Communications."

Marius Pesavento (M'00) received the Dipl-Ing. and M.Eng. degrees from Ruhr-Universitt Bochum, Bochum, Germany, and McMaster University, Hamilton, ON, Canada, in 1999 and 2000, respectively, and the Dr.-Ing. degree in electrical engineering from Ruhr-Universitat Bochum in 2005. Between 2005 and 2007, he was a Research Engineer at FAG Industrial Services GmbH, Aachen, Germany. From 2007 to 2009, he was the Director of the Signal Processing Section at MIMOon GmbH, Duisburg, Germany. In 2010, he became an Assistant Professor for Robust Signal Processing and a Full Professor for Communication Systems in 2013, at the Department of Electrical Engineering and Information Technology, Technische Universitt Darmstadt, Darmstadt, Germany. His research interests include robust signal processing and adaptive beamforming, high-resolution sensor array processing, multiantenna and multiuser communication systems, distributed, sparse, and mixed-integer optimization techniques for signal processing and communications, statistical signal processing, spectral analysis, and parameter estimation. He has received the 2003 ITG/VDE Best Paper Award, the 2005 Young Author Best Paper Award of the IEEE TRANSACTIONS ON SIGNAL PROCESSING, and the 2010 Best Paper Award of the CROWNCOM conference. He is a Member of the Editorial Board of the *EURASIP Signal Processing Journal*, and served as an Associate Editor for the IEEE TRANSACTIONS ON SIGNAL PROCESSING in 2012–2016. He is a Member of the Sensor Array and Multichannel Technical Committee of the IEEE Signal Processing Society, and the Special Area Teams "Signal Processing for Communications and Networking" and "Signal Processing for Multisensor Systems" of the EURASIP.